

Development of a Novel Air Sparging Device

Andrew Reid Hobert

Thesis submitted to the faculty of the
Virginia Polytechnic Institute and State University
in partial fulfillment of the requirements for the degree of

Master of Science
in
Mining and Minerals Engineering

Gerald H. Luttrell
Greg T. Adel
Michael Mankosa

August 28, 2014
Blacksburg, Virginia

Keywords: column flotation, sparging, fine particle flotation

Copyright 2014

Development of a Novel Air Sparging Device

Andrew Reid Hobert

ABSTRACT

Column flotation is commonly employed in the processing and recovery of fine mineral particles due to an increase in flotation selectivity unattainable using conventional flotation methods. Such an increase in selectivity is due to the employment of wash water, minimizing hydraulic entrainment of fine gangue particles, and the presence of quiescent operating conditions assisted by the use of various air sparging technologies. High performance air spargers increase the probability of collision and attachment between air bubbles and particles, thereby improving recovery of fine and coarse mineral particles otherwise misplaced to the tailings fraction in conventional flotation cells. Although many high-pressure spargers, including the static mixer and cavitation tube, are currently employed for the aeration of column cells, a low pressure sparger capable of providing equivalent performance while resisting a reduction in aeration efficiency does not exist.

In light of escalated energy requirements for operation of air compressors necessary to provide high pressure air to existing external and internal spargers, a low-pressure and porous sparger capable of resisting plugging and scaling was developed. Following the design, construction, and optimization of such a prototype, air holdup and flotation performance testing was completed to verify the viability of the sparger as a replacement to existing aerators. Performance evaluations suggest that the sparger is capable of providing similar functionality to currently employed sparging technologies, but further work is required with regards to manipulation of the porous medium to prevent sparger fouling and sustain high aeration efficiencies.

ACKNOWLEDGEMENTS

The author would like to thank his advisor Dr. Gerald Luttrell and boss, Dr. Michael Mankosa, in addition to the entire Eriez Flotation Division, for their unwavering support and direction throughout the duration of this project. Additionally, a thank you is given to Bob Bratton for his assistance and support, and Jim Waddell, whose experience, knowledge, and friendship allowed for this project to be completed.

A special thank you is also given to the author's mother and father who provided continuous support, encouragement, criticism, and love on a daily basis since his birth. He would not be the man he is today without them.

Lastly, and most importantly, loving gratitude is given to his wife Audra who provides encouragement, happiness, and care, making life a much better place.

TABLE OF CONTENTS

ABSTRACT	ii
ACKNOWLEDGEMENTS	iii
TABLE OF CONTENTS	iv
LIST OF FIGURES	v
LIST OF TABLES	vi
1.0 INTRODUCTION	1
1.1 Background	1
1.2 Project Objective	3
2.0 LITERATURE REVIEW	4
2.1 Introduction to Flotation	4
2.2 Column Flotation	6
2.3 Column Flotation Performance	11
2.4 Flotation Sparging	16
2.5 Internal Spargers	17
2.5.1 Low Pressure Perforated and Porous Spargers	17
2.5.2 Single and Two Phase Jetting Spargers	19
2.6 External Spargers	21
2.6.1 Static Mixer/Microcel	21
2.6.2 Cavitation Sparging	24
2.7 Sparger Comparisons	26
3.0 EXPERIMENTAL	30
3.1 Sparger Development	31
3.2 Equipment Setup and Test Work	35
3.2.1 Gas Holdup Testing	35
3.2.2 Flotation Testing	41
4.0 RESULTS AND DISCUSSION	46
4.1 Air Holdup Performance	46
4.2 Flotation Performance	55
5.0 CONCLUSIONS	59
REFERENCES	61
APPENDIX A – 1.6 mm Bead Testing Program	63
APPENDIX B – 1.0 mm Bead Testing Program	67
APPENDIX C – No Magnetic Medium Testing Program	71

LIST OF FIGURES

Figure 1. Conventional Flotation Cell Schematic	5
Figure 2. Rougher, Cleaner, Scavenger Flotation Circuit	6
Figure 3. Flow of Water in a Column Flotation Cell	9
Figure 4. Schematic Illustration of a Single Eriez StackCell	11
Figure 5. Effect of Aeration rate on the Grade and Recovery Curve for a Copper Ore	13
Figure 6. Tracer Study showing the effects of Wash Water Utilization	14
Figure 7. Two Phase Sintered Metal Porous Sparger	19
Figure 8. Eriez SlamJet Sparger	21
Figure 9. Microcel Static Mixer Sparger	22
Figure 10. Microcel™ Process Diagram	23
Figure 11. Eriez Cavitation Tube Sparger	25
Figure 12. Comparison of Performance for Various Spargers	27
Figure 13. Effect of Implemented Sparger Types on Phosphate Recovery	28
Figure 14. Conceptual Diagram of In-Line Magnetic Ring Sparger	31
Figure 15. In-Line Magnetic Ring Sparger	32
Figure 16. MagAir Sparger Prototype Design	33
Figure 17. External Magnetic Flow-Box Sparger Design	34
Figure 18. Horizontal and Vertical Magnetic Sparger Orientation Evaluation	36
Figure 19. Residual Air Holdup Evaluation Test Assembly Set-Up	36
Figure 20. Holding Cell Air Holdup Measurement Method	37
Figure 21. Magnetic Sparger Air Holdup Measurement System	38
Figure 22. 250 x 150 micron Wet Magnetite Media Sample	39
Figure 23. 1.0 mm and 1.6 mm Spherical Magnetic Media	40
Figure 24. Sparger Air Distribution Using 1.0 mm Ferritic Stainless Steel Beads	40
Figure 25. External Magnetic Sparger Flotation Test Assembly	41
Figure 26. Flotation Test Magnetic Sparger Media Housing	42
Figure 27. Flotation of a Minus 150 Micron Coal using Magnetic Sparging System	44
Figure 28. 1.6 mm Beads: Air Velocity (ft/s) vs. Residual Gas Holdup (%) – 18 ppm Frother	47
Figure 29. 1.0 mm Beads: Air Velocity (ft/s) vs. Residual Gas Holdup (%) – 18 ppm Frother	47
Figure 30. No Beads: Air Velocity (ft/s) vs. Residual Gas Holdup (%) – 18 ppm Frother	48
Figure 31. Introduced Air Fraction (%) vs. Residual Gas Holdup (%) – 72 GPM (18 PPM)	52
Figure 32. Introduced Air Fraction (%) vs. Residual Gas Holdup (%) – 81 GPM (18 PPM)	52
Figure 33. Introduced Air Fraction (%) vs. Residual Gas Holdup (%) – 90 GPM (18 PPM)	53
Figure 34. 1.6 mm Beads: Combined Velocity [Water + Air] (ft/s) vs. Air Pressure (psi)	54
Figure 35. Air Flow (scfm) vs. Combustible Recovery (%) with and without a Porous Medium	57
Figure 1-A. 1.6 mm Beads: Air Velocity (ft/s) vs. Residual Gas Holdup (%) – 12 ppm Frother	65
Figure 2-A. 1.6 mm Beads: Introduced Air Fraction (%) vs. Residual Gas Holdup (%) -18 ppm Frother ..	65
Figure 3-A. 1.6 mm Beads: Combined Velocity [Water + Air] (ft/s) vs. Air Pressure (psi)	66
Figure 1-B. 1.0 mm Beads: Air Velocity (ft/s) vs. Residual Gas Holdup (%) – 12 ppm Frother	69
Figure 2-B. 1.0 mm Beads: Introduced Air Fraction (%) vs. Residual Gas Holdup (%) -18 ppm Frother ..	69
Figure 3-B. 1.0 mm Beads: Combined Velocity [Water + Air] (ft/s) vs. Air Pressure (psi)	70
Figure 1-C. No Beads: Introduced Air Fraction (%) vs. Residual Gas Holdup (%) – 18 ppm frother	73
Figure 2-C. No Beads: Combined Velocity [Water + Air] (ft/s) vs. Air Pressure (psi)	73

LIST OF TABLES

Table I – Sparger Flotation Results Without use of Magnetic Beads	56
Table II – Sparger Flotation Results with use of Magnetic Beads.....	56
Table I-A – Sparger Generated Gas Holdup Using 90 GPM Water and 1.6 mm Beads	64
Table II-A – Sparger Generated Gas Holdup Using 81 GPM Water and 1.6 mm Beads	64
Table III-A – Sparger Generated Gas Holdup Using 72 GPM Water and 1.6 mm Beads.....	64
Table I-B – Sparger Generated Gas Holdup Using 90 GPM Water and 1.0 mm Beads.....	68
Table II-B – Sparger Generated Gas Holdup Using 81 GPM Water and 1.0 mm Beads	68
Table III-B – Sparger Generated Gas Holdup Using 72 GPM Water and 1.0 mm Beads	68
Table I-C – Sparger Generated Gas Holdup Using 90 GPM Water and No Beads.....	72
Table II-C – Sparger Generated Gas Holdup Using 81 GPM Water and No Beads.....	72
Table III-C – Sparger Generated Gas Holdup Using 72 GPM Water and No Beads	72

1.0 INTRODUCTION

1.1 Background

Froth flotation is a method of fine particle separation, physical or chemical, which utilizes differences in surface chemistry of minerals within a mineral/water slurry. Flotation is employed for the recovery of valuable fine grained ores, often less than 100 microns in size and either technically or economically unrecoverable by gravity concentration or other separation techniques such as magnetic separation. Through the introduction of air to a liquid pulp, air bubbles selectively adhere to naturally, or chemically altered, hydrophobic minerals and carry those solids to a surface froth phase for removal. Easily wetted, or hydrophilic, material remains in the pulp phase for removal via a tailings or refuse stream. Froth flotation can be performed using an array of established flotation technologies and methods, but is most commonly executed using mechanical and column flotation cells. Conventional froth flotation, also known as mechanical flotation, utilizes a mechanical agitator to disperse air into a mineral slurry using a rotating impeller. Conventional flotation cells are capable of yielding high mineral recoveries when operated in series, but suffer from limited product grades and non-selectivity due to short circuiting of gangue laden feed water, poor recovery of fine particles less than 20 micron, and entrainment of fine waste particles. The efficiency of fine particle flotation using conventional flotation is also poor due to the low probability of collision between fine particles and bubbles.

To solve such issues and improve process efficiencies, column flotation is performed using quiescent countercurrent flows of air and feed slurry in a taller cell to eliminate intense shearing and increase flotation selectivity. The quiescent conditions provided by this flotation method improve the selective flotation of both fine and coarse particles (Luttrell & Yoon, 1993). Downward flowing wash water is also added to the froth phase to minimize the hydraulic

entrainment of fine gangue particles. As a result, column flotation has become widely accepted for its ability to produce higher grade products at increased product yields.

To improve mass recoveries and minimize the misplacement of high grade fine particles to the tailings or refuse stream, column flotation employs a more unique aeration method. Conversely to the employment of mechanical agitation in conventional froth flotation for the aeration of a mineral pulp or slurry, column flotation uses an array of air spargers to introduce a fine upward rising air bubble distribution at the base of a column flotation cell. The introduction of a finer air bubble distribution improves flotation kinetics and increases the total bubble surface area flux, or total available bubble surface area for mass transfer (Laskowski, 2001). Efficient and proper air sparging is vital to the success of column flotation as an increase in bubble size promptly decreases the probability of bubble-particle collision. Existing sparging technologies include, but are not limited to, porous spargers, one-phase and two-phase jetting spargers, hydrodynamic cavitation tubes, and static in-line mixers, many of which are operated using high-pressure compressed air.

Given the significant horsepower requirements necessary to supply compressed air to currently operated high-pressure spargers, a low-pressure sparger operable by use of an air blower offers potentially substantial economic gains. Additionally, the capital cost of an air blower is considerably lower than that of a high horsepower air compressor. Existing low pressure spargers, such as sintered metal porous spargers, are operable at significantly lower pressures, but often suffer from plugging and diminishing performance when introduced to a mineral pulp, thereby reducing sparging efficiency and increasing air pressure demands over time. As a result, the development of a non-plugging, low-pressure sparger capable of providing equivalent metallurgical performance to both existing jetting and dynamic external spargers

would provide both operational and capital cost savings in many global processing beneficiation applications that employ column flotation.

1.2 Project Objective

The objective of this project was to design and develop a low pressure porous sparger capable of resisting a diminishment in performance over extended periods of use in column flotation applications. Such a sparger could be used as an alternative to existing in-line spargers employed in column flotation applications, but would be capable of operation by means of a low-pressure blower. The tasks completed in this research and development project include the design of a low pressure sparger, construction of a sparger with alterable parameters, and completion of an array of test work to verify the viability of the sparger's performance.

The sparger designed in this work effort utilizes magnetism to retain a magnetic media bed through which air is dispersed into a moving slurry. By use of a porous medium, incoming air is distributed and broken into fine air streams before introduction to a recirculated mineral pulp. Similarly to the Microcel design, air bubbles directly contact moving particles to increase the probability of bubble-particle attachment. Magnetism was strictly chosen with a goal of manipulating or rotating the internal magnetic material by movement of external magnets or an alteration in magnetic fields. Although the overall objective of this project was to design a long term non-plugging porous sparger, test work was devoted to proving the viability of the designed sparger as a means of aeration in column flotation processes. This information then makes it possible to test the sparger with several proposed cleaning concepts in both a laboratory and pilot plant setting with knowledge that the sparger is capable of providing sufficient fine and coarse particle flotation performance.

2.0 LITERATURE REVIEW

2.1 Introduction to Flotation

Throughout history, numerous forms of technology or processes have been developed for the separation of minerals by density, size, and chemical properties. To concentrate fine particles unrecoverable by existing technology, mineral flotation was tested and established in the mid 1800's for the separation of minerals using differences in surface chemical properties. Following the initial patenting of a flotation concept used for the separation of sulfides in 1860 by William Haynes, the Bessel brothers designed and constructed the first commercial flotation plant, for the purpose of cleaning graphite minerals, in Germany in 1877 (Fuerstenau, Jameson, & Yoon, 2007). In addition to their innovative use of nonpolar oils to improve the process kinetics of graphite by mineral agglomeration, the Bessel brothers were the first to reportedly use bubbles, resulting from boiling, to increase flotation rates of graphite in water. Flotation continued to develop throughout the late 1800's as multiple methods of sulfide flotation began to expand. For example, in 1898, Francis Elmore patented and implemented a process utilizing oil to agglomerate pulverized ores and carry them to the surface of water for the concentration of sulfide minerals at the Glasdir Mine in Wales (Fuerstenau, Jameson, & Yoon, 2007).

The physical separation or concentration of fine particles by true froth flotation was first utilized in 1905 for the separation of lead and zinc ores from tailings dumps at Broken Hill's Block 14 mine in Australia (Hines & Vincent, 1962). Shortly after, the Butte and Superior Copper Company built the first froth flotation plant in the United States in 1911 (Hines & Vincent, 1962). Due to the success of sulfide flotation in the early 1900's, the use of copper in the United States grew by approximately 5.8 percent annually during that time period (Hines & Vincent, 1962).

Although numerous flotation methods and flotation cells have been developed throughout mineral processing history, the conventional mechanical cell and the column cell are most common in present day mineral processing. The mechanical cell was invented in 1912 and is the most widely implemented or accepted form of flotation today. To aerate a slurry, mechanical cells, as shown in Figure 1, utilize an agitator consisting of a stator and impeller. Air is naturally drawn down the stator or delivered using a low-pressure blower, and dispersed by an impeller which agitates, circulates, and mixes the flotation pulp with the introduced air. As a result of high intensity mixing between air and solids, physical contact between particles and air bubbles occurs.

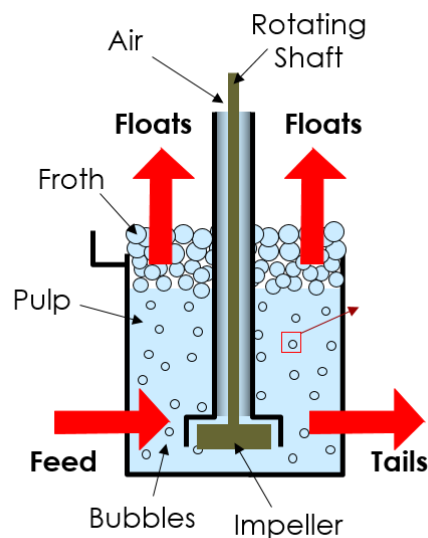


Figure 1. Conventional Flotation Cell Schematic (Luttrell G., *Industrial Evaluation of the StackCell Flotation Technology*, 2011), Used with permission of Dr. Gerald Luttrell, 2014

Mechanical cells are beneficial in that they are capable of treating high material throughputs, but struggle with lower concentrate grades due to short circuiting of feed water to the froth phase and non-selective entrainment of fine particles. To overcome these challenges and improve overall recovery and grade, cells can be operated in series or various flotation circuits can be implemented. For example, in a rougher-cleaner circuit, the concentrate of a

single rougher bank is re-floated to “clean” or refine the product, improving concentrate grade. Additionally, a rougher-scavenger circuit can be implemented to re-float the tailings from the rougher bank to improve overall recovery as high solids loading in a rougher bank can lead to inefficiencies in separation and misplacement of coarser material to the tailings due to froth crowding. Vast circuit configurations consisting of multiple cells and recirculation of material, as shown in the rougher-scavenger-cleaner circuit in Figure 2, provide improved recoveries and higher product grades, but equipment and operational expenditures significantly increase and efficiencies in fine and coarse particle flotation remain low. Due to its ability to improve separation efficiencies, minimize hydraulic entrainment, increase fine particle flotation selectivity, and yield higher product grades, while often requiring fewer flotation cells and reagent volumes, column flotation has flourished in the mineral processing industry.

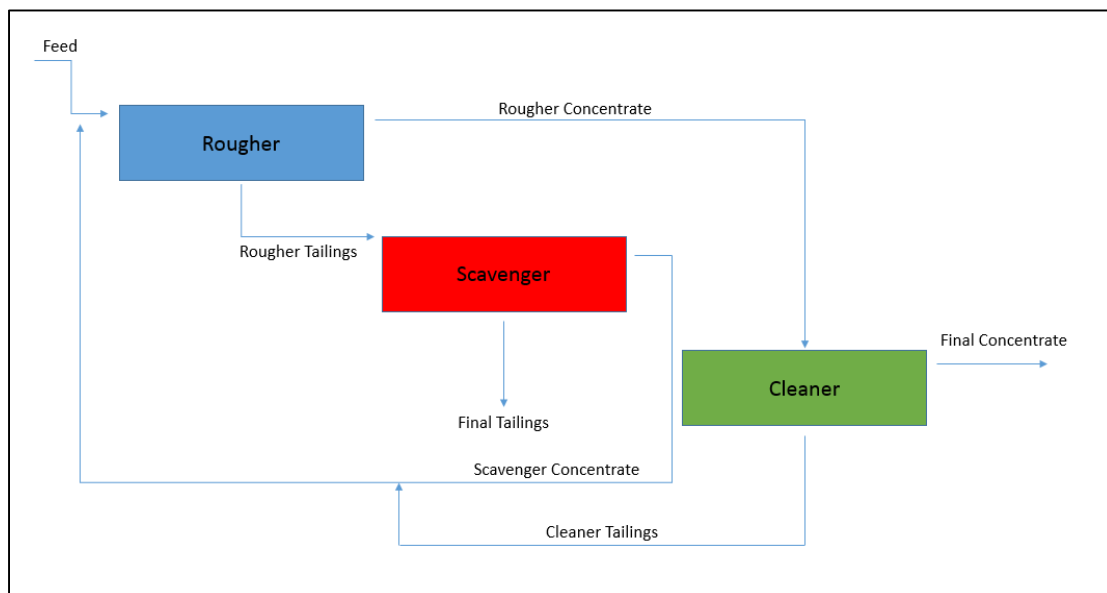


Figure 2. Rougher, Cleaner, Scavenger Flotation Circuit

2.2 Column Flotation

Column flotation is a form of innovative froth flotation that uses the countercurrent flow of air bubbles and solid particles in a pneumatic cell. Pneumatic flotation, performed in a column

like structure with an air sparging device, was first developed by Callow in 1914 and the concept of countercurrent flow of slurry and air within a flotation column was later introduced in 1919 by Town and Flynn, as described by Rubenstein (Rubenstein, 1995). The column flotation concept, as it is known today, was further investigated and patented in the 1960's by Boutin and Tremblay and is currently employed in the roughing, scavenging, and cleaning of valuable minerals such as gold, copper, coal, and zinc (Finch & Dobby, 1990).

Although various forms of column designs were developed in the 1970's and 1980's, including the Hydrochem and Flotaire column cells, the Canadian column was the first to be developed and is the most commonly implemented form of column cell in today's processing applications, as reviewed by Dobby (Finch & Dobby, 1990). The Canadian column was first tested in the late 1960's by Wheeler and Boutin and the first commercial column cell was installed for the cleaning of Molybdenum ore in 1981 at Les Mines Gaspé in Quebec, Canada (Wheeler, 1988). Following its successful application in molybdenum cleaning, the column cell became more widely applied for the flotation of sulfide and gold ores, as well as coal, and the cleaning of copper, lead, zinc, and tin in the late 1980's and early 1990's (Wheeler, 1988). The rapid employment of the Canadian column, and development of the column flotation method, in many mineral processing applications can be attributed to its ability to yield improved product grades, while increasing the recovery of both fine and coarse particles.

Separation of fine particles with high specific surface areas, resulting from crushing and grinding to liberate mineral value, while concentrating a high grade product requires control of hydraulic entrainment of fine gangue particles. In comparison to the flotation performance offered by conventional, mechanically agitated flotation cells, columns yield a higher quality concentrate grade in a single flotation stage due to the removal of entrained fine gangue particles

reporting to the froth through the use of wash water. Wash water showers the froth bed of the column vessel to eliminate entrained gangue minerals that degrade the product grade and replaces pulp that normally reports to the concentrate in conventional flotation methods with fresh water (Kohmuench, 2012). The flow rate of pulp to the froth concentrate must be less than the countercurrent flow of wash water to minimize non-selective recovery of ultrafine gangue (Luttrell & Yoon, 1993). Column cells, as shown in Figure 2, are also built with a smaller cross sectional area to maintain a deeper and more stable froth bed necessary for froth washing. In addition to froth washing and the use of a deep froth, column flotation promotes quiescent operating conditions and utilizes air spargers to improve flotation selectivity and fine particle recovery, respectively.

Unlike conventional flotation cells, taller column cells, reaching up to 16 meters in height to permit necessary particle residence times, utilize high-pressure internal or external spargers for very fine air bubble introduction. Air, or an air/water mixture, is injected at the base of the cell, via an arrangement of spargers, as feed is introduced below the froth bed, developing a countercurrent flow of feed particles and air bubbles. Due to lower traveling velocities of both bubbles and particles during column flotation, collision and attachment between the two are more likely. Increased contact time between air bubbles and particles under quiescent operating conditions decreases the probability of hydrophilic particle attachment. Such conditions also greatly improve coarse particle collection efficiency as coarse particles are less likely to detach from air bubbles under less turbulent conditions present within column cells. Due to the use of wash water and a deeper froth bed, a large quiescent pulp or contact zone, and various air sparging technologies, column flotation presents the most ideal separation environment in a single flotation stage.

Essentially, column flotation presents a multi stage flotation circuit within one cell, illustrated by the development of the Microcel™ by Luttrell et al. (United States of America Patent No. 5761008, 1988). For example, the pulp zone or bubble-particle contacting region represents a rougher stage as hydrophobic particles adhere to air bubbles and are carried to the froth phase in this zone. Additionally, a deep froth and wash water are used to clean the concentrate of hydraulically entrained fine gangue particles to represent the cleaning phase of a multi-state circuit process. Lastly, external air spargers are often utilized to directly introduce air to a circulated tailings stream, scavenging possibly misplaced fine hydrophobic particles. As a result, column flotation is increasingly preferred for the flotation of finer particle size classes to improve recovery and concentrate grade.

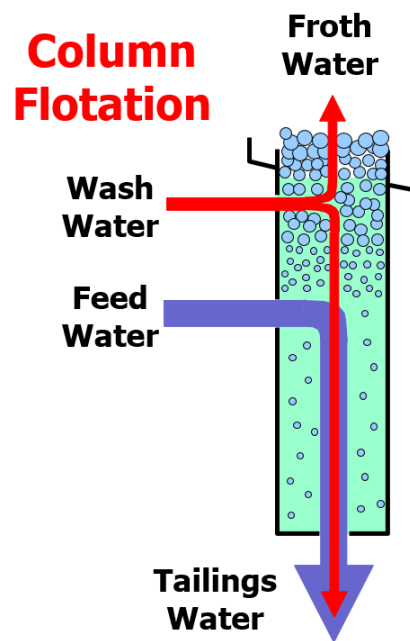


Figure 3. Flow of Water in a Column Flotation Cell (Luttrell G., *Industrial Evaluation of the StackCell Flotation Technology*, 2011), Used with permission of Dr. Gerald Luttrell, 2014

Although column flotation produces superior product grades than those yielded by conventional flotation, consideration must be given to carrying capacity for proper cell design.

Carrying capacity, in pounds or tons per hour per square foot, is the mass rate of floatable solids that can be carried by a given superficial gas velocity. As described by Luttrell, a column cell must be scaled according to its carrying capacity due to an inherently smaller ratio between column cross sectional area and volume when compared to conventional flotation cells (Luttrell & Yoon, 1993). The equation for carrying capacity, in mass rate of concentrate solids per unit of cell area, is as shown:

$$C = 4 Q_g D_p \rho \beta / D_b \quad [1]$$

where β is a packing efficiency factor, ρ is the particle density, D_p is the particle diameter in the froth, D_b is the bubble diameter, and Q_g is the gas flow rate. To achieve optimal carrying capacity conditions, column cell spargers are operated at maximum allowable air velocities, while maintaining the minimum average bubble size. The maximum air flow rate is governed by the bubble size and V_L , or superficial liquid velocity in the cell. Particle residence times are also higher in column flotation due to a taller pulp zone and the naturally slower rise of small bubbles. Given increased particle residence times present using column cells given their geometry, work has been completed to develop flotation technology which offers column-like performance with significantly reduced particle residence times.

In addition to the column cell, further work has been done in recent years by the Eriez Flotation Division to develop an innovative form of flotation technology labeled the StackCell (Kohmuench, Mankosa, & Yan, 2010). The StackCell, as shown in Figure 4, offers column-like performance with shorter particle residence times, improved bubble-particle contacting, and a reduced unit footprint per processed ton of material (Kiser, Bratton, & Kohmuench, 2012). Unlike typical column cells, the StackCell utilizes an aeration chamber to agitate and mix the feed with air in a high intensity shearing zone. By the act of intense agitation, low pressure air,

introduced to the slurry before entrance to the aeration chamber, is sheared into small bubbles for collection of fine particles. High particle concentration and gas fraction within the chamber greatly reduces particle residence times. Additionally, the use of low pressure air and the turbulent environment within the pre-aeration chamber decreases energy requirements as energy is primarily consumed in bubble-particle contacting instead of particle suspension (Kiser, Bratton, & Kohmuench, 2012). The mixture of slurry and air lastly overflows into a short, column like tank, where froth and pulp are separated. A deep froth bed is maintained and froth wash water is employed with the StackCell design to reduce hydraulic entrainment, similarly to column flotation. Due to their compact size and ability to be stacked in unison, stackcells offer much friendlier orientation in a processing plant than column cells, which are much larger and require more structural steel for support and allowance of de-aeration of the froth before reporting to the dewatering circuit (Kohmuench, Mankosa, & Yan, 2010).

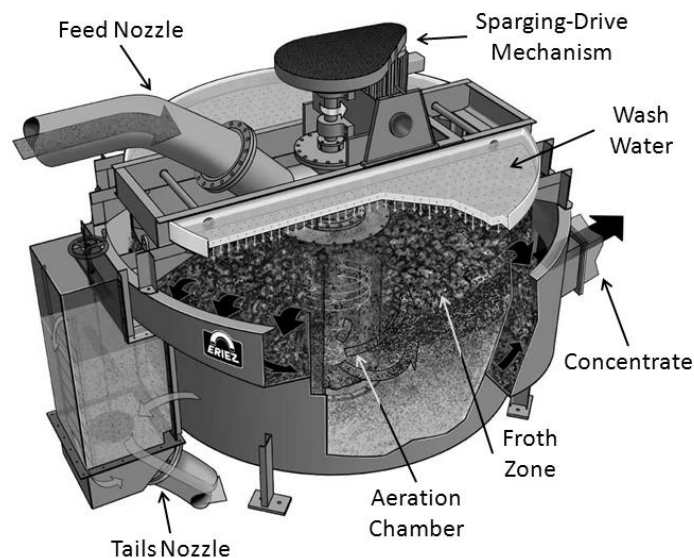


Figure 4. Schematic Illustration of a Single Eriez StackCell (Kohmuench, Mankosa, & Yan, *Evaluation of the StackCell Technology for Coal Applications*, 2010), Used with permission of Dr. Jaisen Kohmuench, 2014

2.3 Column Flotation Performance

Flotation performance is influenced by many factors including froth depth and structure, slurry flow characteristics, flotation cell dimensions, wash water utilization, chemical additions, and gas holdup. Air holdup in a gaseous-liquid mixture is primarily controlled by bubble size or frother dosage, superficial gas velocity, slurry density, and superficial or discharge liquid velocity, as detailed in studies completed by Yianatos et al, and Finch and Dobby (Finch & Dobby, 1990; Yianatos, Finch, & Laplante, 1985). Column cells are typically operated with a 12 to 15 percent gas holdup, or percentage of air in a gaseous-liquid volume. Superficial gas velocity and gas holdup maintain a positive linear relationship, in what is known as the homogenous bubbly flow regime, until gas flow rate becomes too significant (Finch & Dobby, 1990). At this point, air begins to coalesce, bubble size uniformity is lost, and water is displaced to the froth phase.

To illustrate the reaction of a typical flotation bank as gas flow rate is increased, the effect of superficial gas velocity on the recovery and grade curve of a Mt. Isa copper rougher flotation bank is shown in Figure 5. As superficial gas velocity was increased, copper recovery also increased, but copper grade diminished due to increased recovery of gangue material. Although not evidenced in Figure 5, instigation of air coalescence quickly decreases recovery. As stated by Finch and Dobby, development of very large and quickly rising air bubbles will create a churn-turbulent regime within a flotation column as superficial gas velocity exceeds approximately 3 to 4 cm/s (Finch & Dobby, 1990). Coalescence of air quickens the rise of air in a column and increases mean bubble diameter, decreasing total bubble surface area and diminishing bubble-particle collision efficiency.

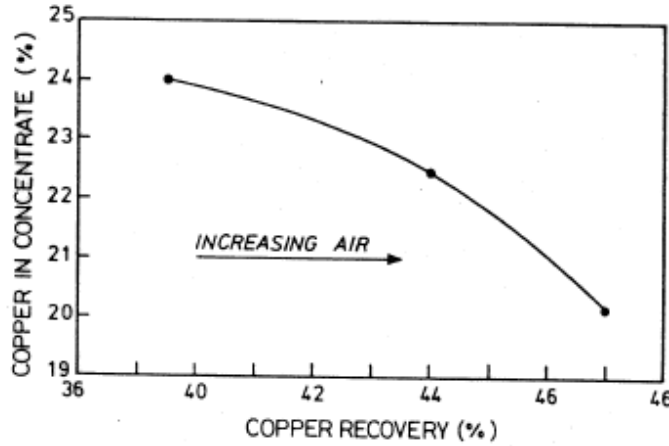


Figure 5. Effect of Aeration rate on the Grade and Recovery Curve for a Copper Ore (Finch, *Mineral and Coal Flotation Circuits*, 1981), Used under fair use, 2014

As gas holdup increases, the probability of bubble-particle collision also increases as the availability of bubble surface area for mass transfer escalates. This is due to a decrease in bubble size or increase in gas flow rate, both of which control the bubble surface area rate, or S_b . The bubble surface area rate is the ratio between superficial gas velocity and bubble sauter diameter. The equation for S_b is as follows:

$$S_b = 6V_g/D_b \quad [2]$$

where D_b is the diameter of bubbles and V_g is the superficial aeration rate (Luttrell & Yoon, 1993). Probability of collision between a particle and bubble is predominantly dependent upon particle diameter, bubble diameter, and bubble Reynolds number. Yoon and Luttrell (1989) derived an equation for collision probability that states that as bubble diameter decreases or bubble Reynolds number increases, the probability of collision between a bubble and particle increases. Their derived equation for probability of collision is written as follows:

$$P_c = \left[\frac{3}{2} + \frac{4Re^{0.72}}{15} \right] \left(\frac{D_p}{D_b} \right)^2 \quad [3]$$

where D_p represents the particle diameter, D_b is the bubble size, and Re is the bubble Reynolds number. As particle size decreases, the probability of collision and attachment between a particle

and bubble also decreases (Yoon & Luttrell, 1989). Ralston et al. also derived mathematical equations which suggest that the probability of bubble-particle attachment decreases if particles are too coarse as air bubbles become unable to retain such heavy particle loads (Ralston, Dukhin, & Mischuk, 1999). Although bubble size must be minimized at a maximum allowable superficial air velocity to increase the probability of fine and coarse particle collision and attachment, hydraulic entrainment of gangue laden water must also be managed to maximize product grade.

During operation of a column flotation cell, proper bias water rates and froth depths must be utilized to minimize hydraulic entrainment. The effect of wash water utilization on the hindrance of short-circuited feed water to the concentrate is shown in Figure 6. As evidenced by the column flotation tracer study displayed in Figure 6 (Left), employment of wash water cultivates a clean interface free of pulp water contamination.



Figure 6. Tracer Study showing the effects of Wash Water Utilization

Bias is a measurement of the percentage of wash water which reports to the pulp; the remainder of water reporting to the froth zone. According to Dobby and Finch (1990), an adequate bias rate and froth depth are essential to control concentrate grade as gas flow rates are commonly maximized to improve column carrying capacity. Although wash water is required to optimize the particle cleaning process, a minimum bias rate is recommended, up to 80 percent of

which should flow to the concentrate, to prevent short circuiting of material to the overflow, maximize capacity, and ensure mobility of the froth (Finch & Dobby, 1990). Insufficient wash water will lead to a reduction in product grade and a concentrate flow rate greater than that of the wash water. In laboratory and pilot scale testing, a froth depth of greater than one half meter is suggested for gas rates exceeding 2 cm/s to diminish the feed water concentration in the froth zone (Finch & Dobby, 1990). In addition to the many column cell operational parameters which effect flotation performance, chemical reagents are most instrumental in the flotation of many naturally hydrophilic materials.

Although some minerals or rock types, such as coal, are naturally hydrophobic, bubble-particle attachment is strongly dependent upon chemical reagents such as collectors, activators, depressants, and pH modifiers. Collectors (anionic, cationic, or nonionic) are used to generate a thin, nonpolar hydrophobic layer around a particle, rendering it hydrophobic. Selection of collector is dependent upon the charge, positive or negative, or the chemical make-up of the mineral to be floated. Activators and depressants are then used to allow or prevent the collector from physically or chemically adsorbing to a mineral surface, respectively. Lastly, and very importantly, pH modifiers are necessary to control the charge of minerals as a minerals' charge often becomes more positive as a solution decreases in pH from alkaline to acidic conditions.

In addition the importance of collectors and other chemical reagents in promoting the development of bubble-particle aggregates, frother type and dosage dictate both bubble size and rise velocity within a flotation cell. Frother can be either a water soluble or insoluble polymer that stabilizes the dispersion of air bubbles in a flotation pulp by decreasing its surface tension. As surface tension declines, bubble population grows and average bubble diameter decreases. Although many frothers have been developed, the two main classes of frother are alcohols and

polyglycols. Polyglycols help to quickly stabilize a froth, while alcohols are used to expedite the increase of gas holdup (Cappuccitti & Finch, 2009). Much work has been performed to generate relationships between gas velocity and gas holdup using numerous frother types and concentrations (Yianatos, Finch, & Dobby, 1987; Finch & Dobby, 1990; Lee, 2002). Typically, as frother concentration increases, in parts per million, mean bubble diameter reduces and gas holdup rises. In addition to the calculation of gas holdup within a laboratory column using a measurement of pressure differential and pulp density, methods of measuring and mathematically estimating bubble sizes using photography have also been developed to better understand the effects of numerous flotation operating parameters (Yianatos, Finch, & Dobby, 1987). Although operational set-points can be altered to impact flotation recovery and grade, the actual method of bubble generation is integral in obtaining desired flotation performance.

2.4 Flotation Sparging

In column flotation processes, internal and external spargers are utilized to introduce and disperse air into a liquid-mineral pulp. Proper sparger design and performance is essential to column flotation as spargers are used control bubble size, air distribution, and air holdup within the flotation column. External spargers are used to aerate a moving slurry which is pumped from a flotation cell bottom and recirculated as a pulp-air mixture to the column; whereas internal spargers inject air or an air-water mixture directly to the flotation cell. External spargers and some internal spargers, such as the Eriez SlamJet, have expedited the development of column flotation as they can be maintained during operation of the column and are easily operated. Since the development of column flotation, numerous spargers have been established and industrialized to improve bubble dispersion, minimize bubble size, decrease operational costs, and reduce maintenance difficulties.

As expressed by Rubenstein (1995), Callow developed the first pneumatic column flotation sparger in 1914 using a perforated metal frame that was wrapped in a woolen cloth. Air was then introduced to a slurry through the covered frame. Many similar spargers were proposed and tested in the early to mid-1900's, but all suffered from plugging, improper distribution of air, and poor reliability. As sparging technologies have rapidly developed and improved in the last few decades, the popularity of column flotation has grown. Although the overall goal of air sparging remains constant for each type of sparger; the design, sparging method, and features vary substantially between sparger types. Due to differences in operating conditions present in a laboratory in comparison to those found in industrial applications, certain low pressure sparging devices are only feasible in a laboratory setting. Though sparging is applied to industries outside of mineral processing, column flotation sparging for the purpose of valuable mineral recovery will be strictly examined in this report. A detailed explanation of the design and operation of existing spargers in mineral flotation applications is provided to illustrate the advancements and differences in column flotation sparging technologies.

2.5 Internal Spargers

2.5.1 Low Pressure Perforated and Porous Spargers

The perforated sparger characterizes the beginning of sparging in a pneumatic flotation cell. Sparging devices developed in the early 1900's for use in pneumatic columns often consisted of a perforated metal frame or structure through which low pressure air was introduced, sometimes inclusive of a porous filter cover. Filter cloth covers were used to generate finer bubble sizes at low pressures, but suffered from fouling or degradation over extensive periods of use. As a result, various materials, such as glass, ceramic, and fabric, have been used in construction of more rigid porous spargers, but the sintered metal sparger has

become the most widely accepted form of porous sparger. This is due to its rigid construction and ability to produce the most uniform dispersion of fine air bubbles of existing low pressure porous aerators. Sintered metal spargers are comprised of powdered metal which has been fused together due to subjection to heat near the metal's melting point (Mott Corporation, 2014). The average pore size of sintered metal spargers ranges from 60 to 100 microns; therefore allowing the production of extremely fine bubbles (Mott Corporation, 2014). Mouza and Kazakis (2007) studied the effects of porous sparger aperture size and found that sintered metal spargers with a smaller average pore diameter have a more uniform porosity and therefore maintain a more even air distribution (Kazakis, Mouza, & Paras, 2007). According to a study performed by the University of Florida, the average diameter of a bubble emitted from a sintered aluminum or stainless steel sparger ranges from 0.7 to 0.9 millimeters (El-Shall & Svoronos, 2001). Although sintered metal spargers are capable of producing a more fine bubble distribution when compared to other internal and external sparging methods, sintered metal spargers likewise possess the inability to resist plugging when exposed to a slurry or pulp in an industrial environment. Such sparging inefficiencies have primarily been documented in wastewater treatment applications and the separation of oil and water.

As reviewed by Rosso (2005), periodic cleaning of fine pore spargers using water and acid is necessary to prevent a rapid performance decline in wastewater treatment applications due to slime plugging. In a study of porous sparger aeration efficiencies in wastewater treatment applications, diminishing sparger performance was obvious in 21 analyzed wastewater facilities (Rosso & Stenstrom, 2005). Porous spargers require filtered air and water to promote successful continuous flotation and minimize performance deterioration, both of which are not feasible in most industrial beneficiation plants. Single and two-phase porous spargers are sometimes applied

in de-inking flotation, wastewater treatment, and in the separation of oil and water, but are primarily used in a laboratory setting in mineral flotation efforts due to uneconomical maintenance requirements. A single phase sintered metal sparger introduces air only through a porous membrane within a column cell, whereas a two phase sintered metal sparger, as shown in Figure 7, injects air through a porous medium surrounding the circumference of a moving stream of water. The aerated liquid then flows into the column or aerated tank.

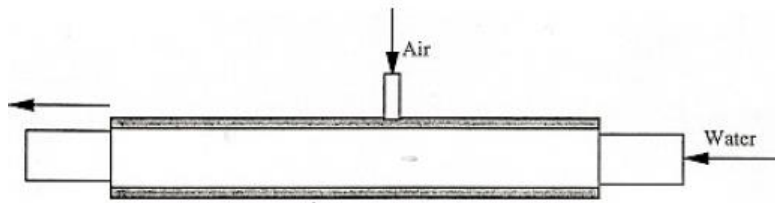


Figure 7. Two Phase Sintered Metal Porous Sparger (*El-Shall & Svoronos, Bubble Generation, Design, Modeling and Optimization of Novel Flotation Columns for Phosphate Beneficiation, 2001*), Used under fair use, 2014

2.5.2 Single and Two Phase Jetting Spargers

In addition to low pressure porous spargers or bubblers, the US Bureau of Mines (USBM), Cominco, and Canadian Process Technologies (CPT) have developed various forms of high pressure jetting internal spargers. In contrast to the operation porous spargers, the jetting action of these high pressure spargers allows for the emergence of numerous air bubbles from a single or multiple orifices with a reduced risk of plugging. Although sparger fouling is less likely at higher pressures, horsepower requirements for the generation of higher air pressures greatly increase operational costs. Cominco and USBM produced the first two phase, high velocity internal sparger that mixes both water and high pressure air before injecting the air/water mixture into the column cell through a perforated pipe. To improve the distribution of water in air, USBM also formulated a model that uses a bead filled mixing chamber to mix water and high pressure air streams. Water addition is used to shear the incoming air, therefore creating a finer

bubble distribution (Finch, 1994). To improve the concept of on-line maintenance, unattainable by USBM and Cominco spargers, CPT later industrialized a single air phase SparJet sparger. The SparJet is a removable air lance that ejects high velocity air from a single orifice through the column wall. Multiple air lances of varying length can be instrumented around the column perimeter to aerate the full cross sectional area of the column. To adjust the air flow through the sparger orifice or to close the orifice in the event of pressure loss, a t-valve is located at the opposite end of the sparger to increase or decrease the total orifice area. CPT later replaced the needle valve with a high tension spring that controls the orifice area depending upon the provided air pressure. The spring is located at the sparger end opposite the orifice and is used to control the position of an internal rod relative to the sparger tip. If air pressure is lost, the spring closes the orifice of the SlamJet to prevent the backflow of slurry into the air system (Kohmuench, 2012).

As detailed by Finch, a long air jet length stretching from the sparger orifice is desired to increase the total population of bubbles. By increasing the density of air by addition of water, the jet length increases and bubbles become finer (Finch, 1994). As a result, EFD enhanced the SlamJet, pictured in Figure 8, with the addition of water as high pressure air and water enter the lance together. Multiple SlamJet spargers consisting of unique orifice sizes exist for any specified flotation duty. The largest SlamJet is operated at pressures in excess of 80 psi for optimal performance in fine coal flotation. The SlamJet sparger is commonly used in flotation of a somewhat coarser feed or deslime circuits which require less collision energy (Kohmuench, 2012). For the flotation of finer particles less than 325 mesh in size, external spargers using direct rapid bubble-particle contacting have been developed.



Figure 8. Eriez SlamJet Sparger (CPT, Canadian Process Technologies, Sparging Systems - SlamJet Series), Used with the permission of Dr. Michael Mankosa, 2014

2.6 External Spargers

2.6.1 Static Mixer/Microcel

Many internal spargers suffer from limited control of bubble size, plugging of openings, low collision energies, and poor on-line maintenance capabilities; therefore the development of external spargers such as the static mixer and cavitation tube have greatly expanded the use of column flotation through the use of microbubbles and picobubbles in mineral processing applications. In the mid 1980's, Luttrell et al. invented and patented the Microcel™ flotation column using a static in-line mixing sparger for the purpose of bubble particle contacting (United States of America Patent No. 5761008, 1988). A static mixer, as shown in Figure 9, is a tube consisting of a series of geometric shapes used as air-slurry mixing components. Potential tailings slurry is removed from the column bottom using a pump and is delivered to a static mixer in addition to high pressure air supplied before the mixer inlet by an air compressor.

Significant air pressure of at least 50 to 60 psi is required for proper operation of industrial scale static mixers to provide 40 to 50 percent air in slurry by volume and to overcome the 20 to 25 psi pressure drop experienced by the air-slurry mixture following its movement through the static mixer. The aerated slurry is then recirculated to the flotation column. Microbubbles generated using a static mixer range from 0.1 to 0.4 mm in size and vastly increase the rate of flotation as bubbles remain small at increased superficial gas velocities (Luttrell,

Yoon, Adel, & Mankosa, 2007). Using a static mixer, high separation efficiencies are realized as a result of a decrease in bubble diameter which increases probabilities of collision and attachment and decreases the probability of bubble-particle detachment.

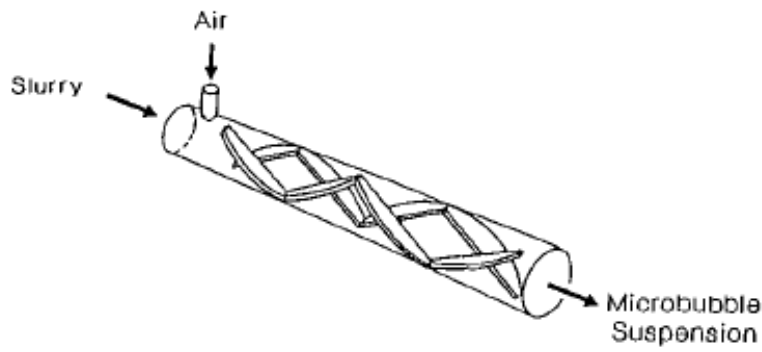


Figure 9. Microcel Static Mixer Sparger (Luttrell, Yoon, Adel, & Mankosa, *The Application of Microcel Column Flotation to Fine Coal Cleaning*, 2007, pp. 177-188), Used with permission of Dr. Gerald Luttrell, 2014

As reviewed by Luttrell (2007), the use of a static mixer, or other external sparging technologies, in column flotation applications allows for the development of a three stage flotation process within one cell (Luttrell, Yoon, Adel, & Mankosa, 2007). This is illustrated by the successful functionality of the Microcel™. As air rises within a flotation column, downward flowing hydrophobic particles collide and attach to air bubbles in the pulp zone in a roughing stage. Risen bubble-particle aggregates are then washed or cleaned in the froth bed to minimize hydraulic entrainment in a cleaning stage. Lastly, the implementation of direct rapid particle contact within a static mixer recycle circuit gives particles a final opportunity for attachment to air bubbles in a scavenger phase. This multi-stage process, as shown in Figure 10, represents a distinct advantage of column flotation that is made possible using external in-line spargers such as the static mixer and cavitation tube.

To demonstrate the value of a static mixer sparging apparatus in the cleaning of fine coal, Luttrell et al. (2007) completed a flotation test program on multiple minus 28 mesh coal samples

using both column and conventional flotation methods. The separation efficiency, or difference between the combustible recovery of coal and ash recovery, was 6 to 16 percent greater using a single twelve inch diameter column equipped with a static mixer than a bank of four, three cubic foot conventional cells (Luttrell, Yoon, Adel, & Mankosa, 2007). In addition to its application in fine coal flotation, the static mixer has also displayed proven performance in coarse particle flotation. In a coarse phosphate flotation study performed at the University of Kentucky (2006), both a static mixer and porous sparger were individually employed for the flotation of a minus 1.18 mm phosphate ore. The effect of a given sparger type on the concentrate grade and total phosphate recovery was determined at varying gas velocities. At the optimum operating point, or elbow of the P_2O_5 recovery and grade curve, established for each sparger, the static mixer provided twelve percent higher phosphate recovery at a slightly better concentrate grade than the porous bubbler (Tao & Honaker, 2006).

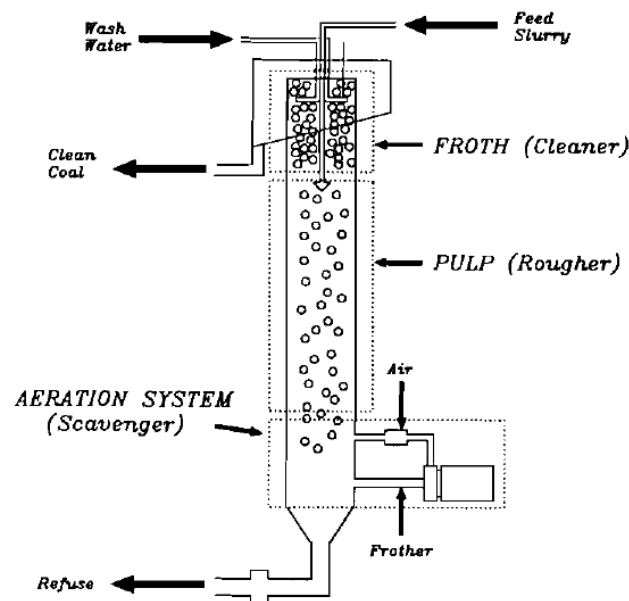


Figure 10. Microcel™ Process Diagram (Luttrell, Yoon, Adel, & Mankosa, *The Application of Microcel Column Flotation to Fine Coal Cleaning*, 2007, pp. 177-188), Used with permission of Dr. Gerald Luttrell, 2014

2.6.2 Cavitation Sparging

In addition to the static mixer, hydrodynamic cavitation based spargers function as in-line aerators utilized in fine particle flotation. Cavitation is the formation of cavities or bubbles within a liquid due to rapid changes in fluid pressure. Bubbles or cavities begin to open up within a liquid at the location of highest fluid velocity where pressure is negative in an attempt to relieve pressure (Zhou, Xu, & Finch, 1993). Such fluctuations in pressure are obtained by the alteration of liquid velocities using a venturi tube configuration. To induce hydrodynamic cavitation in sparging applications, slurry pressure is reduced below its vapor pressure through an area constriction, increasing slurry velocity, and is then returned above its vapor pressure following an increase in slurry flow path cross sectional area. In addition to deviations in fluid pressure, the presence of solid particles and high gas flow rates both help to promote the development of cavities. As discovered by Zhou (1993), high dissolved gas volumes and the addition of frother to decrease the surface tension of a slurry prevent the collapse or implosion of bubbles in the cavitation process, allowing for the successful flotation of fine particles. Using hydrodynamic cavitation, the bubble-particle collision stage is further assisted as bubbles directly form on hydrophobic surfaces immediately during cavitation (Zhou, Xu, & Finch, 1993).

Although several spargers are operable using the principles of hydrodynamic cavitation, the cavitation tube, developed by Canadian Process Technologies, is the most cost effective, high performing, and wear resistant cavitation based sparger. Other spargers which rely upon hydrodynamic cavitation include the eductor and two phase ejector, both of which use a parallel throat and diffuser to promote cavitation, but are not operated in-line with recirculated middlings or tailings streams (El-Shall & Svoronos, 2001). The cavitation tube, as shown in Figure 11, is a completely in-line aerator constructed of a wear resistant material in the shape of an hour glass.

Using an hour glass configuration, slurry pressure is rapidly lowered and increased to support cavitation. Wear resistivity of the inner hour glass lining and the lack of internal mechanisms within the cavitation tube are noteworthy as the static mixer relies upon a series of mixing components in the direct line of slurry flow. Unlike the eductor or two phase ejector, the cavitation tube, now produced by the Eriez Flotation Division, does not employ a feed jet nozzle or air-slurry mixing chamber before entrance to a cavitation inducing structure.

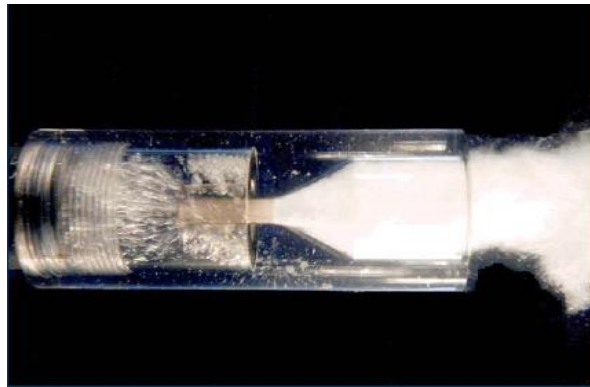


Figure 11. Eriez Cavitation Tube Sparger (*Canadian Process Technologies, Cavitation Sparging System*), Used with the permission of Dr. Michael Mankosa, 2014

Similar to the operation of the static mixer, a pressure drop of approximately 20 to 25 psi occurs across the length of a cavitation tube as a result of rapid modifications in liquid velocity. An operating pressure of 50 to 60 psi is also recommended for industrial applications. As reported by Kohmuench, cavitation tube sparging is common to fine, by-zero, coal circuits that are operated under significant material throughputs as a result of the sparger's ability to formulate numerous bubbles less than 0.8 mm in size (Kohmuench, 2012). The benefits of cavitation and picobubble sparging in fine particle flotation are also evidenced by improvements in product recovery in the flotation of both zinc sulfides and phosphates (Zhou, Xu, & Finch, 1997; Tao & Honaker, 2006). A cavitation tube was used to pre-aerate the feed to a conventional cell and in unison with a static mixer in each scenario, respectively.

2.7 Sparger Comparisons

The air holdup, or percentage of air within an aerated pulp, is directly related to the bubble size generated by a given sparger type and the associated superficial gas velocity. As average bubble size decreases, the air or gas holdup directly increases. Air holdup also increases as a result of an increase in superficial air velocity, until air begins to coalesce. In a study of various sparging technologies conducted at the University of Florida (2001), the performance of multiple sparger types was reviewed under changing operating conditions. Most importantly, the test effort analyzed the effects of increasing superficial air velocity on both the air holdup and bubble size produced by each analyzed sparger. During the sparger performance analysis, a one-phase porous sparger provided the greatest air holdup as gas flow rates were increased, but cavitation based spargers generated the finest bubble sauter diameter, as small as 0.4 mm, at low superficial air velocities (El-Shall & Svoronos, 2001). A complete assessment of the air holdup produced by porous, perforated tube, static mixer, hydrodynamic cavitation based, and jetting spargers as superficial air velocity was increased is shown in Figure 12. As evidenced by this figure, sparging method strongly dictates the relationship between a specified superficial air velocity and resulting air holdup within a flotation column cell.

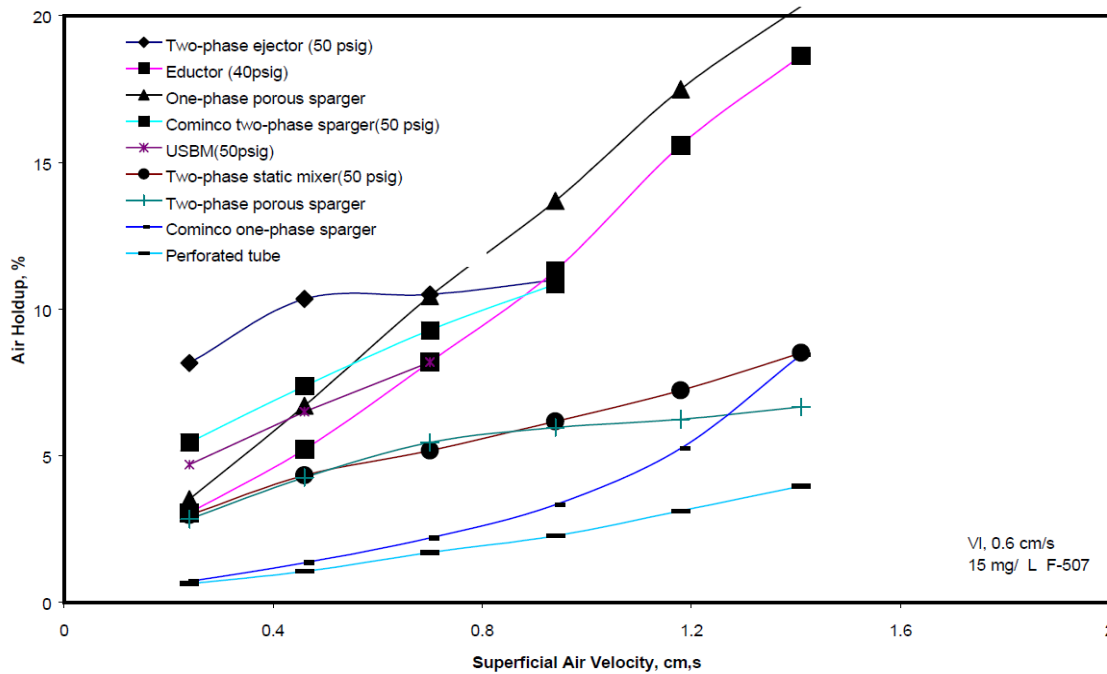


Figure 12. Comparison of Performance for Various Spargers (*El-Shall & Svoronos, Bubble Generation, Design, Modeling and Optimization of Novel Flotation Columns for Phosphate Beneficiation, 2001*), Used under fair use, 2014

In an analysis of the sparging performance generated by the selection of aerators, in terms of air holdup, it is apparent that similar sparging methods provide varying results at increasing superficial air velocities. For example, the one and two phase porous spargers are comprised of an identical porous sintered medium, yet the air holdup generated by the single phase sparger was two to three times greater at increased air velocities due to an escalation in bubble population and lower bubble entrance velocities. In comparison to the two phase porous sparger, the static mixer produced a similar minimum bubble size of 0.7 mm, but at slightly greater gas holdup percentages as air rates were increased. Although the air holdup induced by the static mixer and two phase porous sparger were much less than that of a one phase porous sparger, this study did not consider the effect of increased bubble rise velocities resulting from the use of high velocity fluid flows. It is also possible that an insufficient recirculation liquid velocities were delivered to the static mixer as the superficial air velocity was increased.

Although an in-line cavitation tube was not evaluated in this test effort, other hydrodynamic cavitation based aerators were assessed, such as the eductor and two phase ejector spargers. Each of these cavitation sparging technologies supplied an average bubble diameter and air holdup equivalent to those yielded by a single phase porous sparger. Typically, external spargers provide superior air holdup, fine bubble diameters, and increased bubble-particle contacting necessary to optimize flotation performance, but operational costs are great due to the utilization of significant compressed air volumes. To further support the advantages of both static mixer and cavitation tube technologies, the University of Kentucky conducted a phosphate flotation review using multiple sparger types. As reviewed by the University of Kentucky, the use of a static mixer or cavitation tube to decrease particle detachment increases the recovery of a 16 x 35 mesh phosphate ore considerably (Tao & Honaker, 2006). However, using a single phase porous sparger, phosphate recovery remained significantly lower, as apparent in Figure 13.

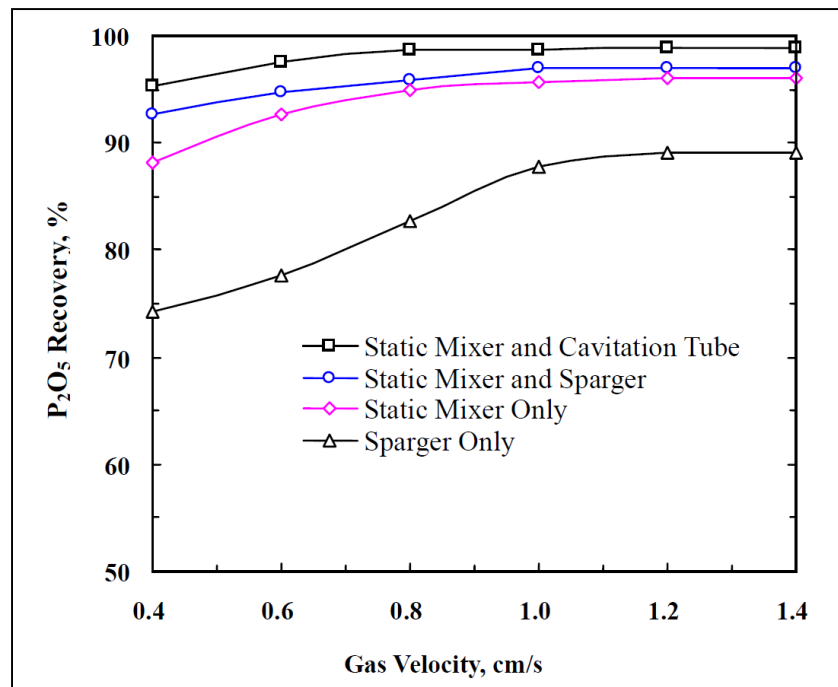


Figure 13. Effect of Implemented Sparger Types on Phosphate Recovery (Tao & Honaker, *Development of Picobubble Flotation for Enhanced Recovery of Coarse Phosphate Particles*, 2006), Used under fair use, 2014

Although currently employed aerators, such as the static mixer, cavitation tube, and SlamJet spargers, are easily operable, non-plugging, and offer increased recoveries of fine and coarse particles, each relies upon high pressure compressed air. To minimize operational costs, a non-plugging, low pressure, and in-line porous sparger capable of sustaining comparable, if not better, flotation performance must be established.

3.0 EXPERIMENTAL

Seeing an opportunity to reduce operational costs associated with column flotation sparging systems, the Eriez Flotation Division designed an innovative low pressure drop sparger capable of resisting plugging and degradation. In design planning of an in-line, non-plugging, and porous sparger, it was determined that magnetic material be employed as a medium through which air be dispersed and introduced to a moving slurry. Such a sparger would maintain an inherently low pressure drop due to the use of a slurry flow path of a uniform cross sectional area and the absence of any in-line mixing components. Alternatively, such a porous sparger would rely upon the dispersion of air through more narrow paths, allowing for the introduction of fine bubble streams from a magnetic media bed. Upon entrance to the flow path, bubble streams would undergo further shearing as a result of high velocity liquid flows. Magnetic material was chosen for the fact it can be manipulated using changes in magnetic fields or movement of host magnets to clean the material during operation. In addition, magnetic material can be structured without need for screens or mesh material to hold the media in place; therefore eliminating the possibility of plugging of apertures through which air must travel. Using the theoretical concept of directing air through a porous magnetic media for the purpose of aerating a recycled slurry stream, a lab-scale magnetic sparger was designed, constructed, and tested at the Plantation Road Facilities in the Mining and Minerals Engineering Department at the Virginia Polytechnic and State University. Although the full scope of the project is to ensure the magnetic material can be cleaned, the first stage of the project was focused on designing of the sparger itself and testing the concept of aerating a slurry through in-line injection of air through a porous magnetic media bed. Before flotation testing progressed, sparger aeration performance was first evaluated under air, water, and frother only conditions.

3.1 Sparger Development

A preliminary prototype was first constructed using a ring magnet assembly, as shown in Figure 14. This approach was first taken to stem from previous research completed by the Eriez Flotation Division, which consisted of aerating a moving coal slurry by the injection of air through the crevices of multiple “in-line” flexible discs. Each disc was identically milled or grooved to promote undeviating aeration of the coal slurry. Although such a novel sparging device yielded both a fine bubble dispersion and high fine particle recovery, grooved air paths began to plug within hours of being subjected to a 15% solids coal slurry. Aperture plugging resulted in a decrease in recovery and air distribution. Using this aeration concept, it was believed that ceramic magnets, protected or layered by a magnetic medium, could be used to alter the previously tested sparger design to prevent the plugging of crevices and create a filter through which air must travel.

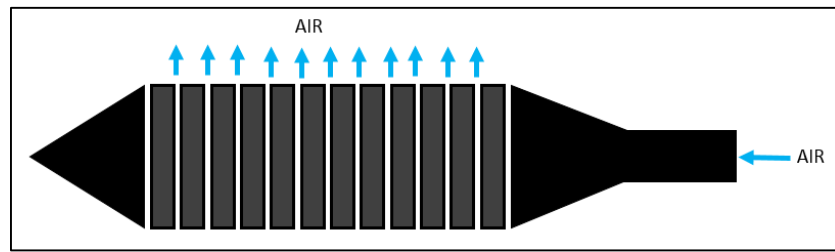


Figure 14. Conceptual Diagram of In-Line Magnetic Ring Sparger

The constructed prototype, inclusive of an inner perforated pipe to introduce air from behind a surrounding group of ceramic ring magnets, is shown in Figure 15. Both ends of the sparger were tapered to allow moving slurry to more evenly flow past the surface of the sparger for uniform aeration. Rubber gaskets were employed at either end of the ring magnet collection, simulating a spring, to allow for expansion of gaps between magnets to support air flow. For the purpose of this effort, sparger air distribution was observed within a clear water tank. Analogous to the performance of the disc sparger, the ring magnet sparger produced a predominantly fine

bubble flux, but air distribution was uneven and large bubbles were frequently emitted from the sparger surface at confined locations due to inconsistent magnet construction and magnetic grit. During limited static water testing, ceramic magnets also became worn quickly, further hampering aeration uniformity.



Figure 15. In-Line Magnetic Ring Sparger

Due to the rapid deterioration of ceramic magnets when introduced to water or high velocity slurries, an improved magnetic sparger was designed to ensure that primary magnetic elements be kept external to slurry or liquid flows in a dry environment. Preservation of magnets external to slurry flow also allows for easier manipulation of magnetic fields or the magnetic medium itself for cleaning purposes. To protect ceramic magnets, improve air distribution, and simplify operation, an external in-line sparging flow box was constructed, as shown in Figure 16. To aerate a recycled slurry or liquid using the designed magnetic sparger, a magnetic medium is held perpendicular to liquid or slurry flows by use of external ceramic magnets as incoming air is dispersed through the medium to dynamically aerate a liquid or solids-liquid mixture. A plexi-glass side housing was used on either side of the sparger to observe the aeration process throughout the testing effort.

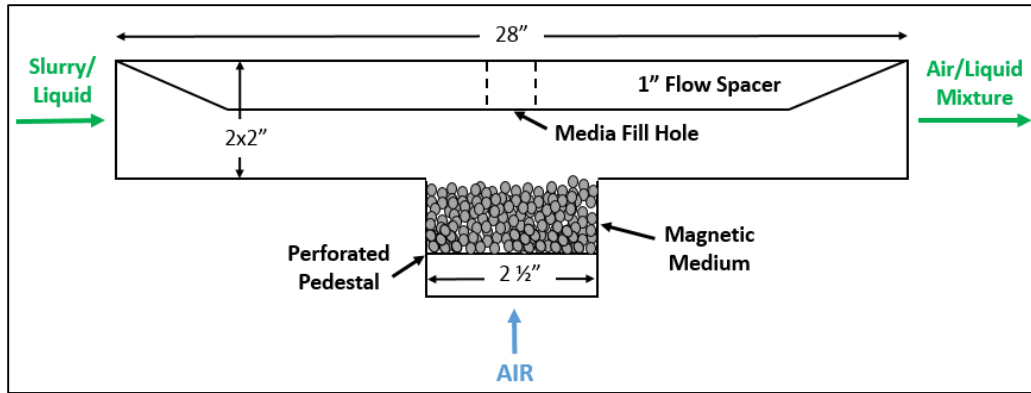


Figure 16. MagAir Sparger Prototype Design

The external magnetic sparger was designed with completely alterable parameters to better understand their effect on sparging performance due to a lack of research or pre-existing information regarding design of such an aerator. These parameters included cross sectional area of the liquid or slurry flow region, magnetic medium bed depth, and magnetic bed area. The sparger, as presented in Figure 17, was assembled with a two inch by two inch cross sectional area and a length of 28 inches. At the sparger's inlet, a 1 ¼ inch pipe nipple and union were utilized to feed the sparger and easily remove it from the testing set-up, respectively. Additionally, a two inch by two inch square pipe was affixed to the outlet end of the sparger in replacement of a succeeding pipe nipple. This allowed a constant cross sectional area to be maintained following the introduction of air to prevent the coalescence of air prior to departure of the aerated liquid from the sparger. A one inch interchangeable spacer, as shown in Figure 17 (left), was also fabricated in order to decrease the cross sectional area of flow to increase the liquid velocity across the magnetic media bed to overcome pumping limitations.



Figure 17. External Magnetic Flow-Box Sparger Design

Within the air inlet chamber perpendicular to the slurry flow region, an adjustable perforated pedestal and slots of fixed height increments were engineered to allow for preparation of a magnetic bed of desired depth. The air chamber was constructed 2 ½ inches in length and assembled equal in width to the flow region (2") to ensure complete and even air distribution across the recirculated slurry or liquid. The perimeter of the perforated pedestal was wrapped in an aluminum tape and caulked to promote air distribution and prevent the short-circuiting of air around the media bed along the chamber walls. Magnetic material was contained by the air inlet compartment and held flush with the liquid flow region boundary by use of two large ceramic magnets on either side of the air chamber, external to the sparging device. Due to the generation of a strong magnetic field, the aluminum pedestal was magnetized and therefore created a level foundation for the media bed to compact and rest upon. Opposite the air pedestal, a threaded magnetic feed hole was created to allow magnetic material to be fed onto the perforated pedestal without needing to disassemble the sparging apparatus. This permitted easier transitions between testing of different media types during aeration performance testing.

3.2 Equipment Setup and Test Work

3.2.1 Gas Holdup Testing

To verify the magnetic sparger's aeration capabilities and optimal operating parameters, a test assembly was developed to quantify the air holdup produced by the sparger under various equipment arrangements and functional conditions. In air holdup testing, water and an MIBC frother were strictly utilized. Mineral slurry or pulp was not employed for these exercises to allow for complete visualization of the process within the sparger and the succeeding de-aeration liquid holding cell. Dynamic external spargers are often operated with a combined air and liquid velocity of 17 to 20 ft/s, therefore a variable speed centrifugal pump was instrumented to produce an array of water flows. Optimal arrangement and installation of the sparger was first defined using a simple recycle system consisting of a 20 gallon sump and centrifugal pump. Both horizontal and vertical sparger orientations were implemented to understand the effect of sparger positioning on air pressure requirements and liquid-air mixing, as shown in Figure 18. Horizontal orientation of the sparger was quickly neglected as air naturally rose and coalesced at the ceiling of the sparger upon introduction through the magnetic medium. A bottom fed vertical orientation promoted the mixture of air and water and decreased the coalescence of air, but increased the air pressure required for aerator operation. Such an increase in air pressure was attributed to an increase in water pressure which acted in opposition to the incoming air. To solve this issue, a top fed vertical orientation was chosen. Using this method, air was more naturally drawn into the liquid flow zone due to the downward flow of a high velocity liquid, significantly decreasing the necessary air pressure by a factor of three to four. Following the selection of an optimal sparger orientation necessary for the aeration of a recycled liquid or slurry, a more complex test

assembly was fabricated to determine the effect of superficial air velocity and recirculated liquid velocity on air holdup.



Figure 18. Horizontal and Vertical Magnetic Sparger Orientation Evaluation

To perform an analysis of sparger performance with regards to air holdup, a test assembly circuit consisting of a primary sump, centrifugal pump, magnetic flow meter, and de-aeration tank was developed. A two dimensional representation of the equipment set-up and flow sheet is illustrated in Figure 19.

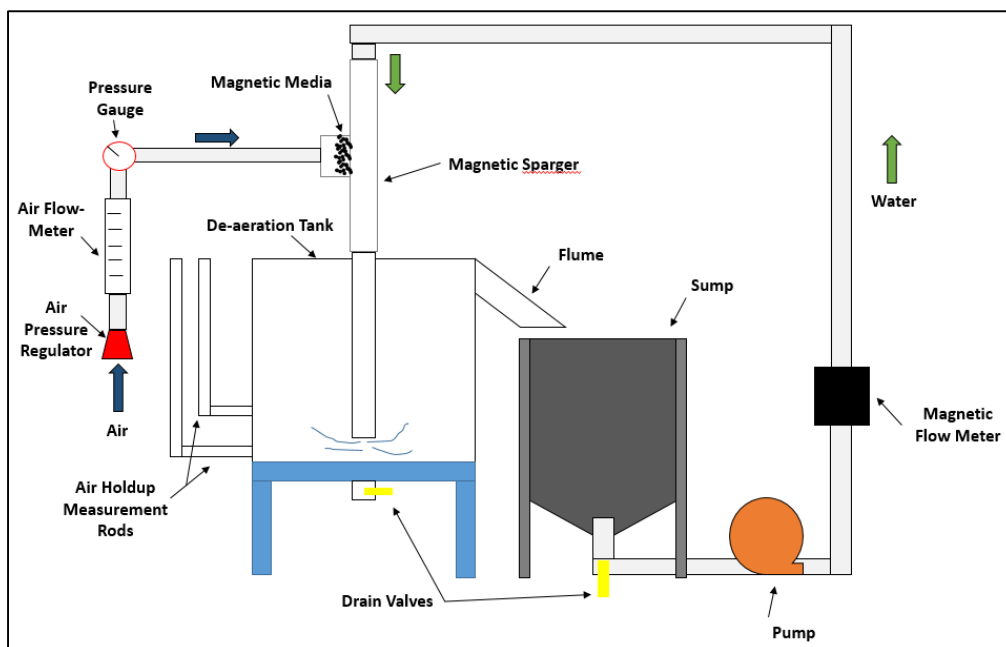


Figure 19. Residual Air Holdup Evaluation Test Assembly Set-Up

A de-aeration tank was applied to the test circuit to increase fluid retention time, increase total fluid capacity, and allow water to de-aerate before recirculation to a feed sump and succeeding variable speed centrifugal pump. In addition, controlled liquid de-aeration in conducted performance evaluations was necessary to properly quantify the air holdup produced by the sparger and to prevent cavitation within the pump head. To determine air holdup, change in liquid elevation within the tank was measured with respect to a fixed measurement port at a known depth of the tank using several elevation rods or measurement tubes. This method of air holdup measurement is illustrated in Figure 20. Using the difference in water elevations determined at transparent measuring ports located just above the sparger outlet inside the tank and below the overflow flume, and the known distance between each port's centers, the percentage of air holdup within the tank was calculated. To ensure accurate and precise measurements were ascertained, level readings were taken at a collection of time intervals and then averaged. To determine the effect of superficial air velocity and recirculated liquid velocity on air holdup, a multi-facet air manifold and magnetic flow meter were employed, respectively.

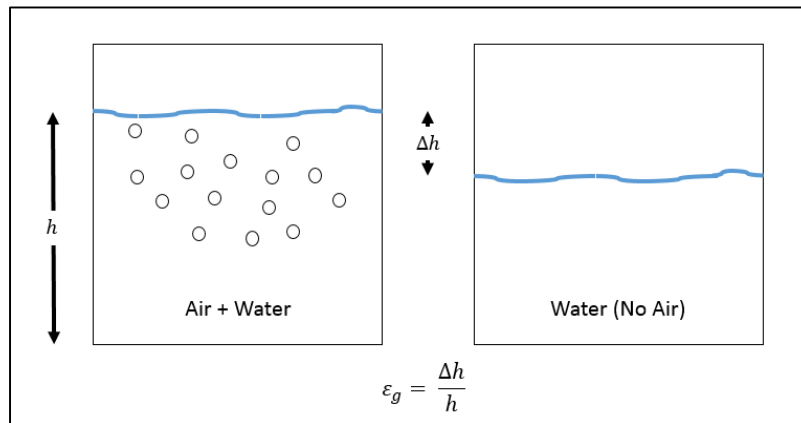


Figure 20. Holding Cell Air Holdup Measurement Method

Compressed air was provided to the experimental system via an air manifold which consisted of a regulator, variable area flow meter, and pressure gauge, as shown in Figure 19 and

Figure 21. Using air pressure and flow rate measurements, the actual air flow rate delivered to the magnetic media bed in standard cubic feet per minute was calculated. Air was supplied to the manifold at approximately 110 psi from a nearby air compressor. In addition to the employment of an air manifold to measure supplied sparger air velocities, a magnetic flow meter was calibrated and utilized to measure water flow rates for each test effort. The maximum water flow produced by the centrifugal pump was approximately 90 gallons per minute. Once steady state air and water flows to the de-aeration tank were obtained, air holdup measurements were taken and recorded using a documented group of sparger operating conditions.



Figure 21. Magnetic Sparger Air Holdup Measurement System

Before air holdup measurements could be taken, sparging operational parameters were chosen and employed. Operational parameters which were altered during testing included:

- Magnetic media type (magnetite, steel shot powder, spherical magnetic media),
- Magnetic medium bed depth,
- Air fraction (percentage of air in water within sparger),
- Cross sectional area of liquid flow region,

- Flow rate of water (gallons per minute), and frother dosage.

Due to the substantial quantity of operational parameters, an optimal magnetic media type was chosen using visual observations. During preliminary evaluations it was concluded that dense magnetite and fine steel shot mediums were incapable of providing a uniform air distribution due to significant compaction of particles upon introduction to water, as depicted in Figure 22. As a result, air quickly short circuited to the perimeter of the impenetrable bed when such forms of media were implemented. Coarse magnetite, crushed in two stages to a size fraction of 1000 x 500 micron, promoted air flow and consisted of particles diverse in shape and size, but increased air distribution variability due to a lack of uniform porosity. Additionally, magnetite and steel shot mediums became oxidized, or rusted, within 24 hours of water submersion, further compacting magnetic particles and obstructing air paths.



Figure 22. 250 x 150 Micron Wet Magnetite Media Sample

To improve air dispersion and maintain a more uniform porous filter medium, a variety of ferritic stainless steel magnetic spheres were employed. A stainless steel coating allows these magnetic spheres to better resist oxidation following extensive subjection to liquid or solids. To perform the testing effort, 1.0 and 1.6 mm magnetic beads, as shown in Figure 23, were utilized.



Figure 23. 1.0 mm (Left) and 1.6 mm (Right) Spherical Magnetic Media

Using a spherical media, distribution of air through the porous bed greatly improved, as displayed in Figure 24. It should be noted that larger bubbles shown in Figure 24 are water droplets external to the sparger housing. Exhausting both sizes of magnetic material individually, sparger testing was performed at varying liquid velocities and gas injection rates. An array of tests were also conducted when no magnetic medium was employed to demonstrate the effect of the porous medium on air holdup.

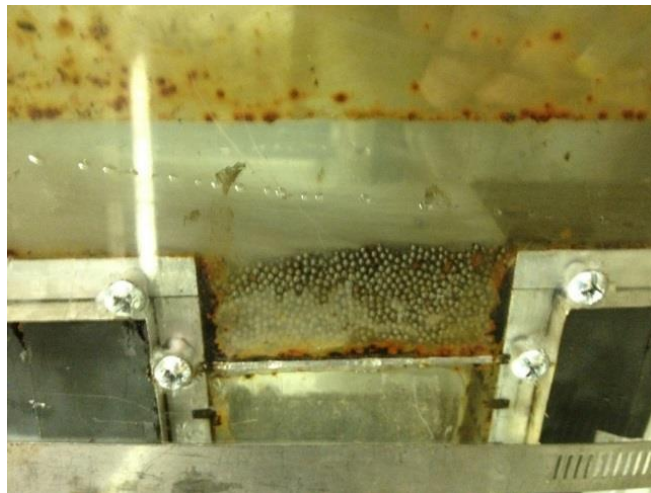


Figure 24. Sparger Air Distribution Using 1.0 mm Ferritic Stainless Steel Beads

3.2.2 Flotation Testing

Succeeding the completion of air holdup evaluations, optimal sparging parameters determined throughout the air holdup test effort were utilized in a laboratory scale flotation study. To complete flotation testing, a minus 150 micron coal sample with a feed ash content of 20 percent by weight was utilized. The feed coal sample, roughly four percent solids by weight, was removed from a 55 gallon drum using a siphon as the tank was thoroughly agitated. To obtain a representative sample, the siphon was guided across the full cross sectional area of the drum. To conduct a continuous flotation test program using the obtained sample, an all-inclusive flotation assembly was constructed using a multi-level steel and wood shelving unit, as displayed in Figure 25.

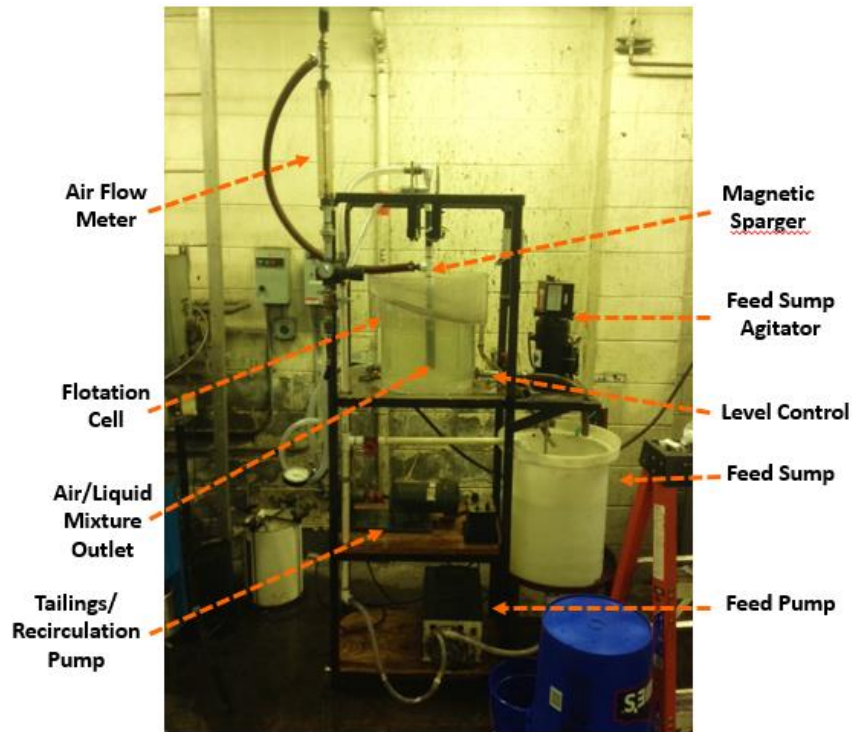


Figure 25. External Magnetic Sparger Flotation Test Assembly

The primary components of the assembled flotation system included a small ten gallon flotation cell, 15 inches in diameter, with an affixed froth launder and a combined feed and

tailings sump. A variable speed peristaltic pump was used to pump feed material, flotation concentrate, and recycled tailings slurry at a rate of two gallons per minute from the sump to the external porous magnetic sparger. A rate of two gallons per minute permitted the necessary mixing or residence time within the sump and was sustained to maintain a consistent pulp-froth interface level. In addition to this mixture of slurry streams, a high velocity refuse slurry stream, removed from the lowermost zone of the flotation cell by use of variable speed centrifugal pump, was delivered to the recessed sparging unit from above at approximately 14 gallons per minute to simulate a column flotation cell external sparging arrangement. Together, these slurry streams provided the required downward constant traveling fluid velocity to the sparger air interface. The aerated coal slurry was lastly injected at the cell bottom. Due to the scale of this test, a smaller form of the magnetic sparger was fabricated using a hose barb inherent of an inlayed perforated screen and two external ceramic magnets used to retain the magnetic media, as shown in Figure 26. Compressed air was delivered from behind the magnetic bed using a $\frac{3}{4}$ " air-line.



Figure 26. Flotation Test Magnetic Sparger Media Housing

Laboratory flotation testing was carried out at an external sparging slurry flow rate of 16.38 gallons per minute. This flow rate was chosen to solicit similar combined air and slurry velocities implemented in previously conducted air holdup evaluations and industrial external sparging applications. To establish a grade and recovery curve for a minus 150 micron coal sample using the magnetic sparger prototype, the provided aeration rate, or air flow rate, was varied from 0 to 2 cubic feet per minute (cfm) using a variable area rotameter affixed to the assembly frame. As air rate was increased, combustible recovery also increased. Air rate was limited to no greater than 2 cubic feet per minute during the test effort to sustain an air fraction, or percentage of air within the aerated recycle stream, of less than 50%. Given a 0.45 in² cross sectional area of the recirculated tailings and feed line, an air flow rate greater than approximately 2 cfm would have yielded an air fraction in excess of 50 percent and produced excessive burping within the flotation cell. Such burping or air bubble coalescence increases the misplacement of water to the froth launder and decreases bubble particle collision and attachment. To identify the maximum air fraction allowable, gas flow rate was increased until substantial disturbance of the froth was visualized as a result of the coalescence of air or burping.

In addition to the variance of aeration rate to control air holdup within the flotation cell, Methylcyclohexanemethanol, or MCHM 8-carbon alcohol frothing agent, was supplied to the feed sump at an addition rate of 10 parts per million (ppm) by volume to decrease the surface tension of the slurry and promote the development of smaller air bubbles. Wash water was not employed in this test program, but an insignificant flow of water was added in the froth launder to provide mobility to the dry froth concentrate to promote drainage and circulation to the feed sump. Minimal water flow was provided to the launder to help maintain the circuit feed percent solids and prevent frother dilution. In an attempt to uphold a constant froth level, a manual gate

valve was located and controlled opposite the high velocity tailings outlet in substitution of a loop controlled pressure transmitter and bladder valve combination. Slurry removed from this valve was deposited in the feed sump below.

Following the designation of an aeration rate at a constant tailings recirculation and feed pumping rate, the flotation cell was operated until a steady state process was achieved. Holding a froth level within the cell was proven difficult due to a lack of visibility of the pulp-froth interface given the short height of the cell, turbulence within the cell, and size of the launder, as presented in Figure 27. Once steady state conditions were assumed, samples of the concentrate and tailings were taken for equal time durations using two gallon buckets of documented weights. This process was conducted at five aeration rates to determine the effect of gas flow rate on combustible recovery and concentrate ash content using the magnetic sparger. Additional operating points on the grade and recovery curve were identified without using magnetic material in the sparger air inlet to verify the effect of the employment of a porous medium on flotation performance.



Figure 27. Flotation of a Minus 150 Micron Coal using a Magnetic Sparging System

Following the collection of samples for each performed steady state grade-recovery scoping test, slurry wet weights were measured and recorded. Slurry samples were then filtered using a vacuum disc filter and dried in an oven at 100° Celsius in preparation for ash analysis. To conduct an ash analysis of all tailings and concentrate samples, an ash analyzer was employed to superheat each sample to over 600° Celsius to burn off all existing combustible particulate. At the conclusion of the superheating procedure, the remaining mass of each sample was representative of each sample's respective ash content. For each steady state test completed, the mass yield to the concentrate and assays of the tailings and concentrate samples were used to calculate the combustible recovery and feed ash content for a given set of operating parameters.

4.0 RESULTS AND DISCUSSION

4.1 Air Holdup Performance

Residual gas holdup or aeration performance evaluations were conducted using two MIBC frother concentrations, 12 and 18 ppm by volume. In most industrial flotation applications, the employment of additional reagents, such as collectors and extenders, also alter the surface tension of a liquid or pulp; therefore higher concentrations of MIBC frother were utilized in this test effort in their absence. For each designated frother addition rate and media size, 1.6 mm, 1.0 mm, or 0 mm, the gas holdup within the succeeding de-aeration holding cell was measured as the sparger air rate was increased to determine the effect of aeration rate on air holdup. Air velocity was varied from 3 to 15 ft/s for three recirculated liquid flow rates of 90, 81, and 72 gallons per minute to also define the relationship between recycled liquid velocity and air holdup. A liquid flow rate range of 72 to 90 gpm, or 11.5 to 14.5 ft/s, was chosen to produce similar liquid velocities implemented in industrial external sparging applications. In addition, air velocities were maintained between 3 and 15 ft/s to ensure a sparger air fraction range of 20 to 50%. Liquid and air velocities were calculated using the geometry of the main sparger flow region, 2 in². The maximum operating air pressure observed throughout all test programs was approximately 6 psi at a combined air and water velocity of 28.6 ft/s. The presence of a magnetic medium negligibly increased air pressure by up to 0.25 at the greatest air velocities. Using air holdup measurements collected at increasing air velocities for each of three liquid velocities, air velocity was plotted versus air holdup for each individual liquid flow rate.

Tabulated data and graphs depicting the effect of increases in air and liquid velocities on air holdup during the employment of 1.6 mm magnetic beads, 1.0 mm magnetic beads, and without magnetic media at a frother dosage of 18 ppm are shown in Figures 28, 29, and 30,

respectively. The effect of air velocity on air holdup at increasing liquid velocities when using 12 ppm of frother was also evaluated and is illustrated in Appendices A, B, and C. As evidenced by the air velocity and gas holdup relationships depicted in Figures 28-30, the gas holdup produced by the magnetic sparger increased proportionally to air velocity equally no matter the media type or liquid flow rate. Given a minimal top to bottom ratio of liquid velocities utilized, $1 \frac{1}{4}$, the effect of the recycled liquid rate on generated air holdup was difficult to identify.

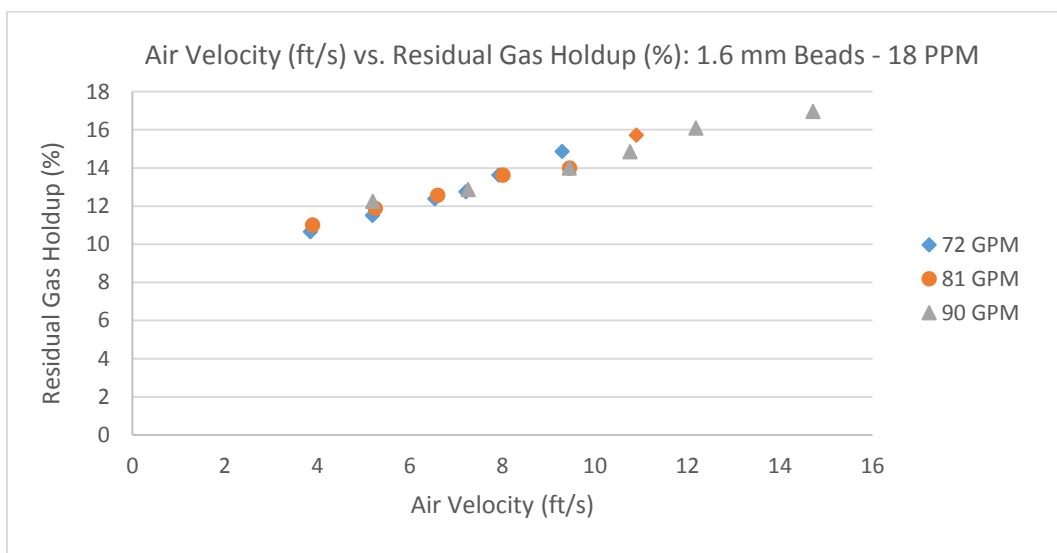


Figure 28. 1.6 mm Beads: Air Velocity (ft/s) vs. Residual Gas Holdup (%) – 18 ppm Frother

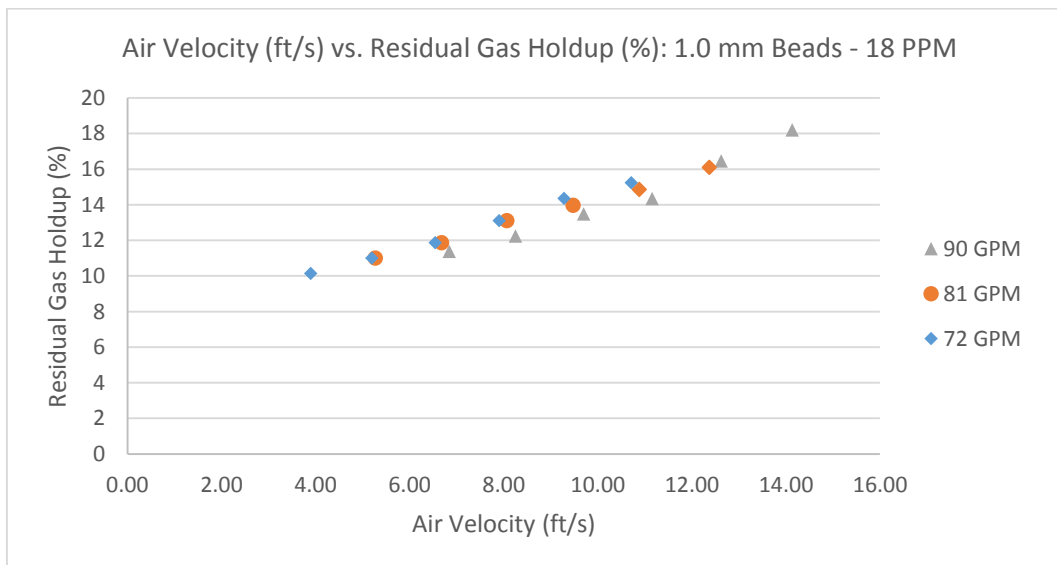


Figure 29. 1.0 mm Beads: Air Velocity (ft/s) vs. Residual Gas Holdup (%) – 18 ppm Frother

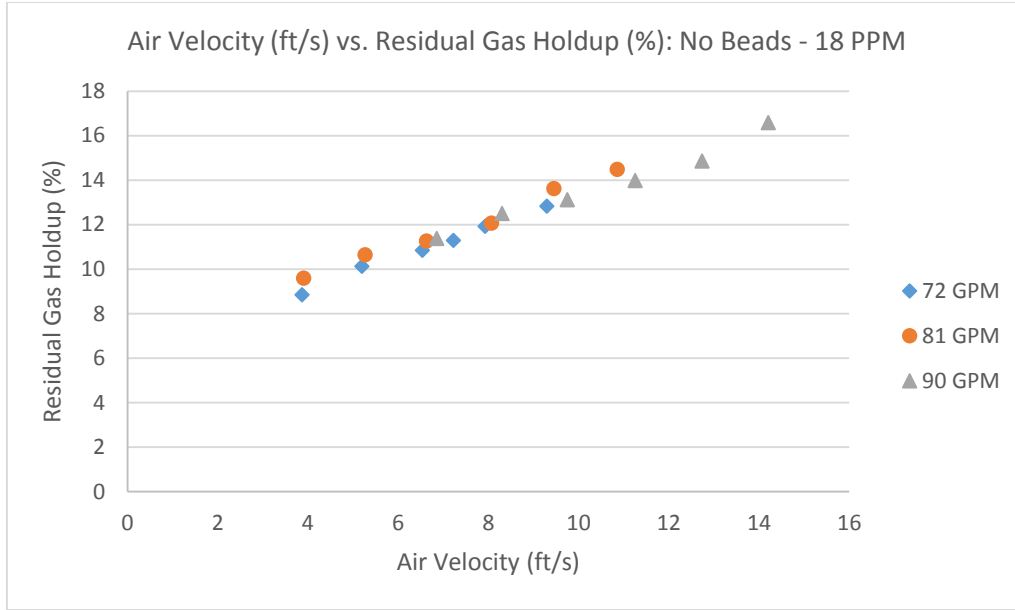


Figure 30. No Beads: Air Velocity (ft/s) vs. Residual Gas Holdup (%) – 18 ppm Frother

For a given air addition flow rate, gas holdup did not significantly differ as liquid velocity was increased due to the limited range of liquid velocities employed and an increase in bubble rise velocity within the holding cell. As liquid velocity was increased, bubble rise velocity also increased, therefore decreasing the measured gas holdup. If much lower liquid velocities were assessed, it is possible that a difference in the yielded air holdup for a specified aeration rate could be more easily distinguishable. To illustrate the effect of bubble rise velocity on gas holdup, a population balance around the de-aeration tank was formulated to calculate bubble rise velocity as liquid velocity was increased. The derivation for bubble rise velocity is shown in equations 4 through 7 and is as follows:

$$\text{Volume Entering Tank} = \text{Volume Escaping Tank} \quad [4]$$

$$(Q_G + Q_L)(\varepsilon_i) = (Q_G + Q_L + u_b A)(\varepsilon_g) \quad [5]$$

$$\varepsilon_g = \frac{(Q_G + Q_L)}{(Q_G + Q_L + u_b A)} (\varepsilon_i) \quad [6]$$

$$u_b = \frac{\frac{(Q_G + Q_L)(\varepsilon_i)}{(\varepsilon_g)} - (Q_G + Q_L)}{A} \quad [7]$$

where Q_G is the gas flow rate, Q_L is the liquid flow rate, ε_i is the air fraction of the introduced or incoming aerated liquid, ε_g is the air holdup within the holding cell, A is the cross sectional area of the tank, and u_b is the bubble rise velocity. As shown in equation 6, air holdup is dependent upon air, liquid, and bubble rise velocities. As air flow rate is increased, air holdup increases, whereas air holdup decreases as liquid and bubble rise velocities increase. This is because retention time of air within a tank or de-aeration cell decreases as the introduced liquid flow rate is increased. Using the derived equation for bubble rise velocity, air rise velocity was calculated for each completed test, as depicted in data summary tables in the attached Appendices.

To demonstrate that smaller air bubbles were generated at greater recycled liquid velocities due to an increase in bubble shearing, bubble rise velocities were analyzed for an equivalent introduced air fraction at increasing liquid velocities. Firstly, air fraction was plotted versus air holdup at increasing liquid flow rates, as shown in the Appendix for each testing effort. Although these relationships indicate that air holdup was nearly equal for a given air fraction at increasing liquid flows, bubble rise velocity greatly increased as liquid flow rates increased. For example, at an air fraction of 40%, the air holdup yielded by the magnetic sparger during the employment of a 1.6 mm bead porous medium was nearly 14% at variable liquid velocities. As liquid flow rate was increased from 72 to 90 gpm, bubble rise velocity increased by 1.25 ft/min. In conclusion, lower air bubble rise velocities present at decreased liquid flow rates yielded air holdup values equivalent to those provided at increased liquid flow rates where the average bubble diameter was smaller. At increased liquid velocities, air arose more quickly within the holding cell, but a greater air shear rate at the liquid to air interface generated bubbles much smaller in size.

Although it is difficult to differentiate the aeration performance of the sparger while operated at varying liquid flow rates, the air holdup provided by the magnetic sparger at combined air and liquid velocities employed in industrial external sparging applications is quite distinguishable. A summary of air holdup values produced at increasing combined liquid and gas velocities and frother addition rates for each testing effort is provided in Tables I, II, and III in Appendices A, B, and C. For example, using a 1.6 mm spherical media diameter, the air holdup within the holding cell increased directly proportional to the combined air and water velocity. Using a frother addition rate of 18 ppm, and a combined air and water velocity of approximately 18 feet per second, the air holdup measured within the tank was 12.75 percent. Such an operating point is similar to that employed in an industrial setting. As liquid flow rate was increased using a 1.6 mm magnetic spherical media, the air holdup realized at the burping point also increased to as great as 14.85 percent. Although gas holdup increases as liquid velocities increase, an understanding of pumping economics is necessary to determine an economical operating point of the sparger.

In addition to the understanding of sparger performance under varying operating conditions while employing a single porous media type, comparison of performance using differing media yielded a recognizable difference in the sparger generated gas holdup, as represented in Figures 31 through 33. To distinguish the difference in performance of the sparger during the employment of each media type or lack thereof a porous medium, introduced air fraction was plotted versus residual gas holdup for each liquid flow rate utilized. As shown in Figure 31, the use of a 1.6 or 1.0 mm magnetic bead porous medium increased gas holdup by almost two percent at a water rate of 72 gallons per minute. To show the effect of liquid velocity or flow rate on this difference, similar data was plotted for liquid flow rates of 81 and 90 gallons

per minute, as shown in Figures 32 and 33, respectively. As liquid flow rate was increased, the difference in air holdup produced with or without magnetic media was less distinguishable, but still evident. Using 81 gallons per minute of water and a bead size of 1.6 mm, air holdup remained almost two percent greater than without the implementation of magnetic media. In contrast, the difference in air holdup reduced to one percent at combined air and water velocities greater than 25 feet per second as realized when using a liquid flow rate of 90 gallons per minute, as shown in Figure 33. This is most likely due to an increase in the shearing effect at the air and liquid interface.

In a comparison of the air holdup performance yielded by each magnetic medium, the 1.6 mm magnetic bead medium continuously produced slightly greater air holdup values than the 1.0 mm bead medium. Because both media types were similar in size, it is difficult to classify the effect of media size on aeration performance. However, preliminary selection of a porous medium did evidence that the use of a uniformly sized porous media is beneficial in the production of a more even air distribution and minimization of short circuited air flows. From optical inspection, the larger media size yielded an improved average air holdup due to an increase in the coalescence of air following its departure from the magnetic bed when using a reduced size of bead. When using a smaller spherical media type, the porosity within the bed remains equal, approximately 26 percent according to a face centered cube lattice, but ejected air streams are located more closely which inherently heightens the risk of coalescence. It is possible that an increase in magnetic bead size could improve air distribution, but bubble size would be expected to increase as well.

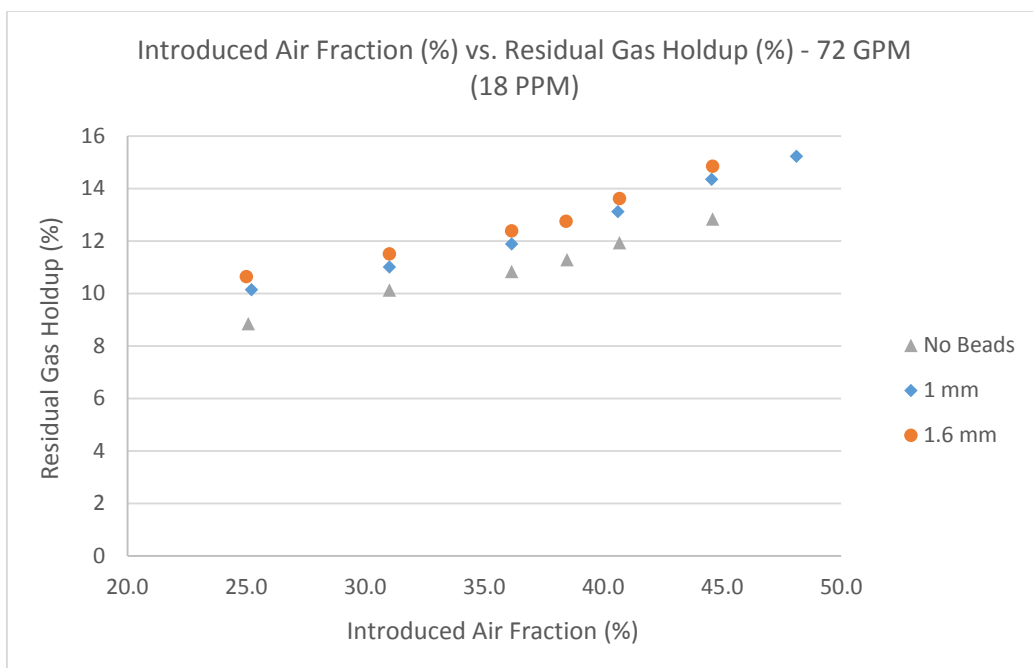


Figure 31. Introduced Air Fraction (%) vs. Residual Gas Holdup (%) – 72 GPM (18 PPM)

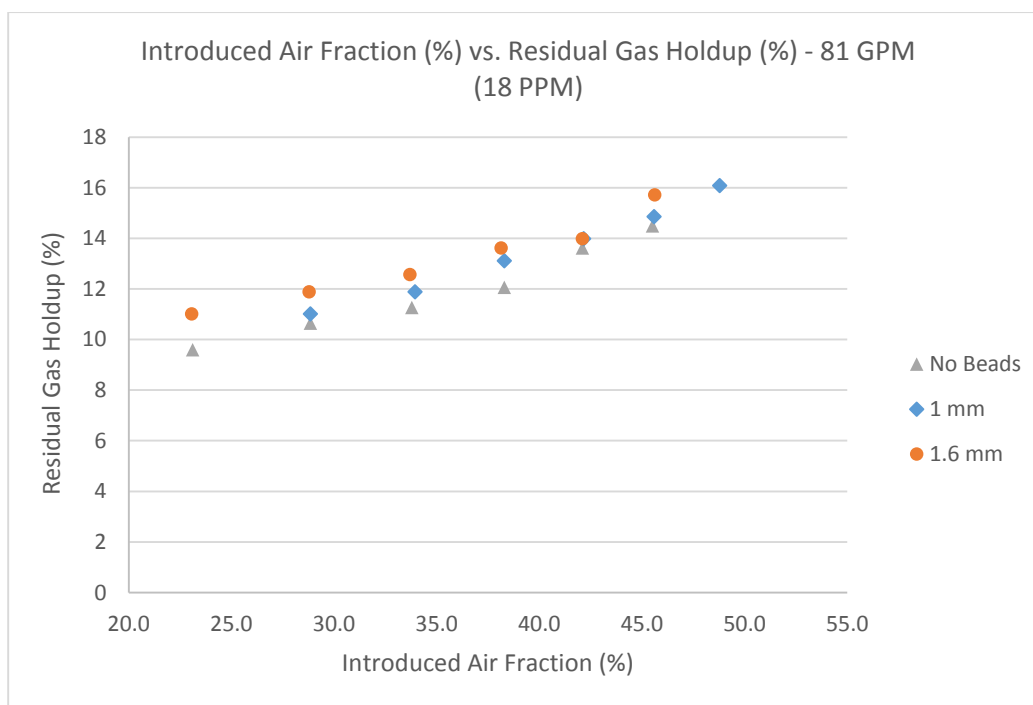


Figure 32. Introduced Air Fraction (%) vs. Residual Gas Holdup (%) – 81 GPM (18 PPM)

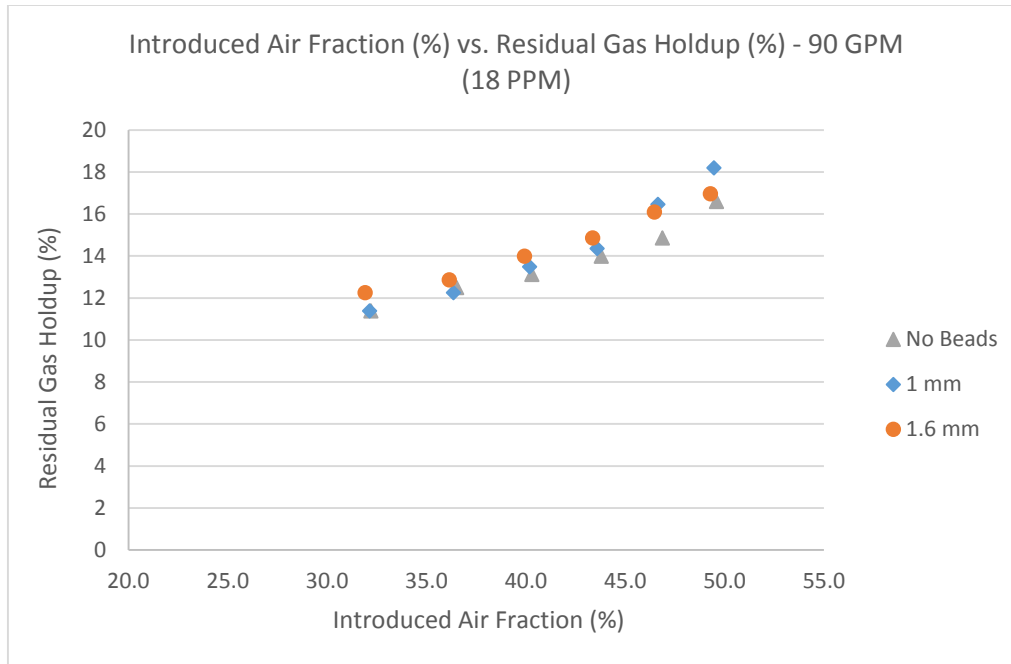


Figure 33. Introduced Air Fraction (%) vs. Residual Gas Holdup (%) – 90 GPM (18 PPM)

Air holdup evaluations demonstrate that an external porous magnetic sparger using this design concept is a capable and economical sparging device in terms of air dispersion and distribution, and air pressure requirements. According to gathered results, air holdup percentages generated by the magnetic sparger using each media type are quite comparable to those provided by currently employed sparging technologies, but at much lower air pressures. As shown in Figure 34, the air pressure required to operate the sparger during the employment of a 1.6 mm magnetic bead porous medium did not surpass 6 psi at a combined air and water velocity greater than 30 ft/s. At this air pressure, a low horsepower blower can be utilized to supply necessary air flow rates. A similar trend in the relationship between the combined velocity of air and water and air pressure was realized in all testing efforts. Necessary air pressures at increasing combined air and water velocities during the implementation of 1.0 mm magnetic beads and no magnetic beads are further detailed in the Appendices B and C.

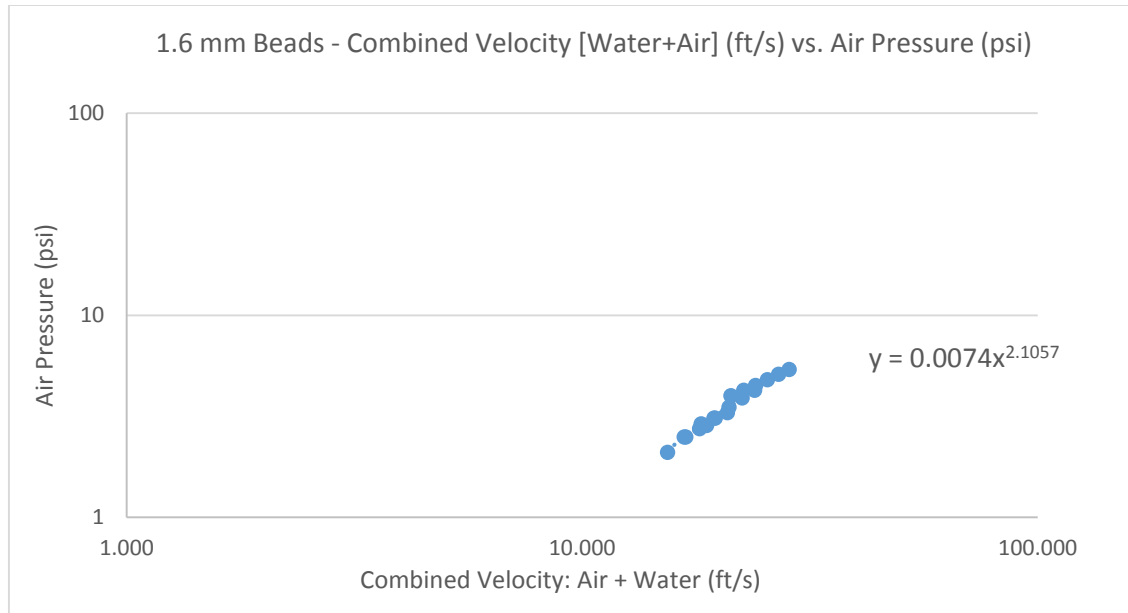


Figure 34. 1.6 mm Beads: Combined Velocity [Water + Air] (ft/s) vs. Air Pressure (psi)

Due to a reliance upon low pressure air, the dimensions of the magnetic bed and the fluid flow region must be properly engineered to minimize required air pressure and promote air distribution. From optical observations of air flow through each tested magnetic medium, the depth and geometrical dimensions of the bed strongly governed the distribution of air at the air inlet. Using a deeper porous bed, air more easily short circuited to a confined location of the bed, thus a minimum bed depth of one inch was utilized. During industrial operation of the sparger, perfect compaction and distribution of material retained at the air inlet will more likely be difficult when a deep bed is maintained. Air pathways increase in size throughout the bed as bead size increases, therefore an increase in bed depth is less detrimental to air distribution. An increase in the width of the bed also increased the short circuiting of air. This was evidenced by the collection of air flow on the low pressure outlet side of the bed at increased fluid pressures. Naturally, air will flow to the path of least resistance where acting pressure is lowest. For the construction of an industrial unit prototype, air inlets should be fabricated with a small cross sectional area of approximately 1.0 square inch or less and a width to depth ratio of

approximately 1.5 to 1.0 to prevent the short circuiting of air. Using multiple air inlets in series as described across the flow region would increase the complete air distribution from the bed and ensure proper aeration of a moving slurry. To prevent the short circuiting of air to the perimeter of the bed, the surfaces of surrounding air inlet walls should be textured roughened to establish similar friction present between individual magnetic beads. The height and hydraulic diameter of the fluid flow region should also be minimized to increase the mixing of air and slurry and to limit the water pressure internal to the sparger to decrease air pressure requirements, respectively.

4.2 Flotation Performance

In addition to the completion of air holdup and aeration performance evaluations, flotation scoping tests were conducted to demonstrate the sparger's ability to yield high mineral recoveries of a finely sized coal sample. Testing was conducted with and without the use of a magnetic porous medium to characterize the benefit of using such material. Steady-state flotation tests were performed at a fixed feed rate as aeration rate was increased from approximately 0.5 to 2.0 scfm to define the relationship between sparger air fraction and mineral recovery. A fixed slurry feed rate of 16.38 gpm, or approximately 12 ft/s, was sustained to reproduce recirculated liquid rates utilized in air holdup evaluations. Once steady-state conditions were established for a given air velocity, samples of the froth concentrate and tailings were procured. An ash analysis was then conducted on each sample to determine their respective ash contents. Ash content values were then employed to calculate the combustible recovery realized for each assumed air flow rate and pressure.

The combustible recoveries and concentrate ash contents achieved at variable air addition rates, with and without the employment of a porous magnetic medium, are displayed in Tables I

and II, respectively. Using the mass yield to the concentrate and ash contents of both the tailings and concentrate fractions, a feed ash content was also back calculated for each test. As evidenced by the flotation test data, combustible recovery improved by up to 20% as aeration rate was increased to an air fraction of nearly 50% by volume. As expected, an increase in air flow rate also increased the average concentrate ash content due to an increase in the hydraulic entrainment of high ash slimes or fines. Given the small volume of the employed flotation cell and limited particle residence time, combustible recoveries yielded during the employment of a porous medium can be considered favorable.

Table I – Sparger Flotation Results Without use of Magnetic Beads

No Beads - Sparger Flotation Results							
True Air (scfm)	Pressure (psi)	Slurry Flow (gpm)	Air Fraction (%)	Feed Ash (%)	Tail Ash (%)	Con Ash (%)	Combustible Recovery (%)
0.51	0.75	16.38	18.97	15.86	21.41	5.66	39.54
1.03	1.00	16.38	32.06	20.02	24.65	9.13	33.92
1.30	1.25	16.38	37.28	18.52	25.77	8.98	48.22
1.57	1.50	16.38	41.83	16.93	25.30	8.04	53.66
2.13	2.00	16.38	49.32	16.71	27.74	9.64	66.12

Table II – Sparger Flotation Results with use of Magnetic Beads

1 mm Beads - Sparger Testing							
Air (scfm)	Pressure (psi)	True Air (scfm)	Slurry Flow (gpm)	Air Fraction (%)	Feed Ash	Tail Ash	Con Ash
0.50	0.75	0.51	16.38	18.97	12.32	21.44	7.62
1.00	1.00	1.03	16.38	32.06	16.38	25.24	9.32
1.50	1.50	1.57	16.38	41.83	16.11	26.29	13.60
2.00	2.00	2.13	16.38	49.32	17.21	34.98	11.86

In addition to the effect of increased aeration rate on recovery, the employment of a 1.0 mm magnetic bead porous medium also greatly improved combustible recovery. Using equivalent air flow rates in both test programs, the utilization of a porous magnetic bed increased combustible recovery by 15 to 25%, as illustrated by the air rate versus combustible recovery

plot illustrated in Figure 35. For example, at an air addition rate of 2.13 scfm, the use of a porous medium increased combustible recovery by 15%. Such an increase in recovery resulted from the production of a finer air bubble distribution, which improved the likelihood of collision and attachment between air bubbles and fine particles. Due to an increase in combustible recovery using a porous medium, yielded concentrates were of a much higher ash content. If a taller column cell had been utilized to increase particle retention time, while also boasting the use of a deep froth and wash water, a more satisfactory concentrate grade and combustible recovery could have been achieved.

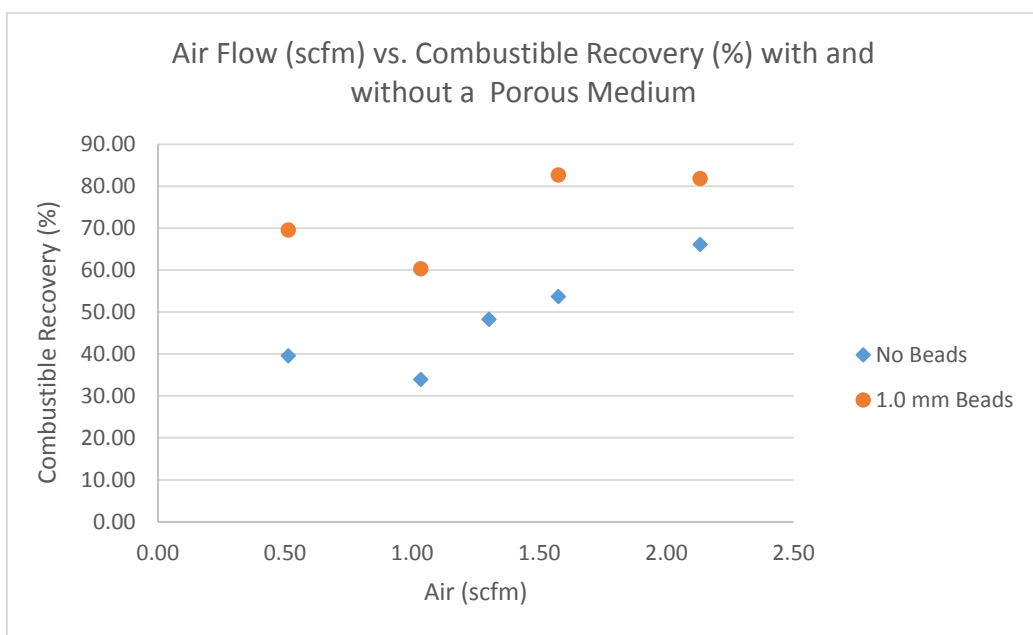


Figure 35. Air Flow (scfm) vs. Combustible Recovery (%) with and without a Porous Medium

Although an improvement in flotation performance was observed during the employment of a porous medium, inconsistencies in calculated combustible recoveries and measured ash contents are apparent. Most importantly, the calculated feed ash did not remain continuous throughout all test work. This was most likely due to inefficient steady state sampling resulting from difficulties experienced in upholding the froth level within the flotation cell by use of a gate

valve at lower aeration rates. Although material was frequently removed from the system, a proper test should sustain a more fixed feed ash content. Due to the size of the sparging prototype, the maximum allowable air addition rate also hindered the development of a more stable froth at lower sparger air fractions. In column flotation applications, approximately 4 scfm of air per square foot is required to aerate the cell. In this study, a maximum of 2.13 scfm was allowable before burping commenced. To appropriately aerate the flotation cell utilized, a one inch recirculation pipe should have been exercised. Such an increase in sparger size would have increased the permissible air addition rate at both low and high air fractions. Although experimental faults were realized, this study demonstrates the value of a porous medium for its ability to increase recovery as a result of an increase in air holdup. To more fully understand the sparging capabilities of the magnetic porous sparger, a laboratory column cell, incorporating wash water and a loop controlled pressure transmitter to maintain a froth level, must be employed.

5.0 CONCLUSIONS

The engineered and performance evaluated low pressure porous sparger demonstrated itself as a viable sparging prototype in terms of bubble generation and distribution, and flotation performance. The air holdup provided by the sparger, ranging from 12 to 16 percent, was similar to that generated by current industrially employed external spargers, such as the static mixer, at comparable combined air and liquid velocities. Due to the presence of a negligible pressure drop at the air-to-liquid interface, the magnetic porous sparger was also capable of yielding such air holdup values at much lower air pressures of 5 to 7 psi. As a result of low operating air pressures, this sparger is operable by means of a low horsepower blower, reducing operational costs significantly.

Following the completion of numerous sparging assessments, practical sparger operating parameters, such as a proper porous medium, correct sizing of the chosen media, necessary combined velocities of air and water, orientation of the sparger, and required air pressure were determined. Because air travels to the path of least resistance, a round magnetic media with a bulk uniform porosity is necessary to avoid the short circuiting of air streams to the perimeter of the porous medium or confined locations of the magnetic bed. To provide complete dispersion of air through the magnetic medium, air inlets with a diameter of 1.5 inches or less, and a bed width to depth ratio of 1.5 to 1.0 are also recommended. Subsequently, a top-fed, vertical orientation of the sparger was deemed optimal to more naturally draw air into the sparger at lower air pressures.

In addition to the identification of ideal sparger operational parameters, conducted aeration evaluations also confirmed the improvement of the aeration of a recycled liquid or slurry by use of a porous magnetic medium. During the employment of a porous magnetic medium in both air holdup and flotation performance test efforts, an increase in air holdup of up to 2 to 3%

and an increase in combustible recovery of a minus 150 micron coal by an average of 15%, respectively, were realized. Although preliminary test results portray the magnetic sparger as a capable aerator, comparative flotation studies must be performed using existing spargers to fully evaluate the prototype. To directly compare the flotation performance of a magnetic porous sparger to currently exhausted industrial sparging technologies, laboratory scale column flotation evaluations, exercising wash water, level control, and a constant frother addition rate, must be executed using both forms of technology. If recognized as a practical replacement to pre-existing external spargers, further investigative efforts with regards to the cleaning of the magnetic medium will be required to inhibit fouling of the porous membrane.

REFERENCES

- Canadian Process Technologies. *Cavitation Sparging System*. Delta, B.C.: CPT.
- Cappuccitti, F., & Finch, J. (2009). Characterization of Frothers and its role in Flotation Optimization. *SME*.
- CPT. *Sparging Systems - SlamJet Series*. Delta, BC: Canadian Process Technologies.
- El-Shall, H., & Svoronos, S. (2001). *Bubble Generation, Design, Modeling and Optimization of Novel Flotation Columns for Phosphate Beneficiation*. Gainesville, Fl: Florida Institute of Phosphate Research.
- Finch, J. (1981). *Mineral and Coal Flotation Circuits*.
- Finch, J. (1994). Column Flotation: A Selected Review-Part IV: Novel Flotation Devices. *Minerals Engineering, Volume 8*, 587-602.
- Finch, J., & Dobby, G. (1990). *Column Flotation*. New York: Pergamon Press.
- Fuerstenau, M., Jameson, G., & Yoon, R. (2007). *Froth Flotation: A Century of Innovation*. Denver, Co: SME.
- G. Luttrell, R. Y. (1988). *United States of America Patent No. 5761008*.
- Hines, P., & Vincent, J. (1962). *The Early Days of Froth Flotation*.
- Kazakis, N., Mouza, A., & Paras, S. (2007). Experimental Study of Bubble Formation at Metal Porous Spargers. *Chemical Engineering Journal*.
- Kiser, M., Bratton, R., & Kohmuench, J. (2012). StackCell Flotation - A New Technology for Fine Coal Recovery. In B. A. M.S. Klima, *Challenges in Fine Coal Processing, Dewatering, and Disposal* (pp. 79-94). SME.
- Kohmuench, J. (2012). Column and Nonconventional Flotation for Coal Recovery. In B. J. Mark S. Klima, *Challenges in Fine Coal Processing, Dewatering, and Disposal* (pp. 186-209). SME.
- Kohmuench, J., Mankosa, M., & Yan, E. (2010). Evaluation of the StackCell Technology for Coal Applications. *International Coal Preparation Congress*.
- Kulkarni, A. (2011). Design and Selection of Sparger for Bubble Column Reactor. *Chemical Engineering Research and Design*.
- Laskowski, J. (2001). *Coal Flotation and Fine Coal Utilization*. Vancouver BC: Elsevier.
- Lee, J.-E. (2002). *A Study of the Bubble Properties in a Column Flotation System*. HydroLab Institute.
- Luttrell, G. (2011). Industrial Evaluation of the StackCell Flotation Technology. *Coal Prep*. Lexington, Ky.

- Luttrell, G., & Yoon, R. (1993). Column Flotation - A Review. In B. Moudgil, *Beneficiation of Phosphate - Theory and Practice* (pp. 361-369). Littleton, CO: SME.
- Luttrell, G., Yoon, R., Adel, G., & Mankosa, M. (2007). The Application of Microcel Column Flotation to Fine Coal Cleaning. *Journal of Coal Preparation and Utilization*, 177-188.
- Mott Corporation. (2014). *Sparging Design Guide and Part Selection*. MOTT.
- Ralston, J., Dukhin, S., & Mischuk, N. (1999). Inertial Hydrodynamic Particle-Bubble Interaction in Flotation. *International Journal of Mineral Processing*.
- Rosso, D., & Stenstrom, M. (2005). Economic Implication of Fine-Pore Diffuser Aging. *Water Environment Research, Volume 78*.
- Rubenstein, A. (1995). *Column Flotation*. CR Press.
- Tao, D., & Honaker, R. (2006). *Development of Picobubble Flotation for Enhanced Recovery of Coarse Phosphate Particles*. Lexington, Ky: Florida Institute of Phosphate Research.
- Wheeler, D. (1988). Column Flotation - The Original Column. In *Developments in Mineral Processing, Vol. 9*. Elsevier.
- Yianatos, J., Finch, J., & Dobby, G. (1987). Bubble Size Estimation in a Bubble Swarm. *Chemical Engineering Science*.
- Yianatos, J., Finch, J., & Laplante, A. (1985). *Estimation of Local Holdup in the Bubbling and Froth Zones of a Gas-Liquid Column*. Chemical Engineering Science - Elsevier.
- Yoon, R., & Luttrell, G. (1989). The Effect of Bubble Size on Fine Particle Flotation. *Mineral Processing and Extractive Metallurgy Review*, 101-122.
- Zhou, Z., Xu, Z., & Finch, J. (1993). One the Role of Cavitation in Particle Collection During Flotation. *Minerals Engineering, Vol 7*, 1073-1084.
- Zhou, Z., Xu, Z., & Finch, J. (1997). Role of Hydrodynamic Cavitation in Fine Particle Flotation. *International Journal of Mineral Processing*, 139-149.

APPENDIX A – 1.6 mm Bead Testing Program

Table I-A – Sparger Generated Gas Holdup Using 90 GPM Water and 1.6 mm Beads

2 in² - 90 Gal/Min (14.5 ft/s) Water - 1.6 mm Beads						
SCFM Air	Air Pressure (psi)	A + W Velocity (ft/s)	Air Fraction (%)	Gas Holdup - 12 PPM (%)	Gas Holdup - 18 PPM (%)	Bubble rise Velocity (ft/min)
10	5.4	28.47	49.28	16.09	16.96	12.27
9	5.1	26.97	46.47	14.85	16.09	11.52
8	4.8	25.49	43.37	13.62	14.85	11.07
7	4.5	24.04	39.93	12.75	13.99	10.09
6	4.25	22.61	36.15	11.88	12.87	9.25
5	4	21.20	31.91	11.01	12.25	7.70

Table II-A – Sparger Generated Gas Holdup Using 81 GPM Water and 1.6 mm Beads

2 in² - 81 Gal/Min (13 ft/s) Water - 1.6 mm Beads						
SCFM Air	Air Pressure (psi)	A + W Velocity (ft/s)	Air Fraction (%)	Gas Holdup - 12 PPM (%)	Gas Holdup - 18 PPM (%)	Bubble rise Velocity (ft/min)
8	4.25	23.89	45.6	14.85	15.72	10.27
7	3.9	22.44	42.1	13.62	13.99	10.20
6	3.5	21.01	38.1	12.75	13.62	8.55
5	3.1	19.60	33.7	11.51	12.57	7.45
4	2.9	18.25	28.8	10.65	11.88	5.87
3	2.5	16.89	23.1	9.78	11.01	4.17

Table III-A – Sparger Generated Gas Holdup Using 72 GPM Water and 1.6 mm Beads

2 in² - 72 Gal/Min (11.5 ft/s) Water - 1.6 mm Beads						
SCFM Air	Air Pressure (psi)	A + W Velocity (ft/s)	Air Fraction (%)	Gas Holdup - 12 PPM (%)	Gas Holdup - 18 PPM (%)	Bubble rise Velocity (ft/min)
7	3.3	20.85	44.6	13.21	14.85	9.44
6	3.1	19.47	40.7	11.93	13.62	8.75
5.5	2.85	18.76	38.4	11.03	12.75	8.55
5	2.75	18.09	36.1	10.84	12.38	7.85
4	2.5	16.74	31.0	9.23	11.51	6.41
3	2.1	15.40	25.0	8.85	10.65	4.69

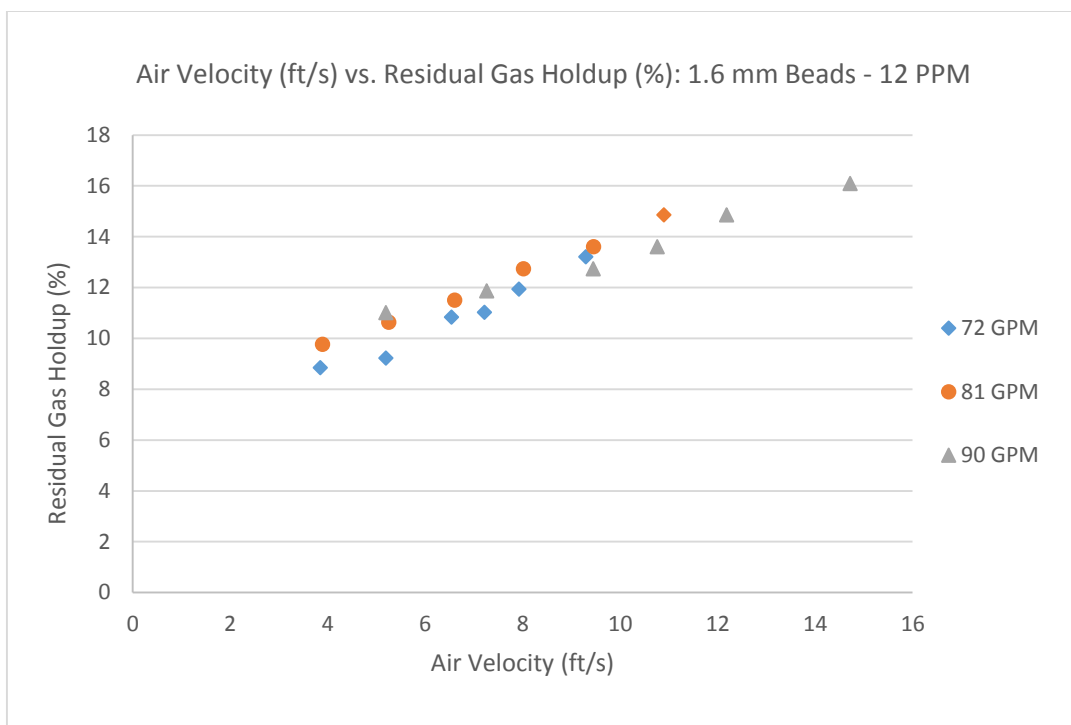


Figure 1-A. 1.6 mm Beads: Air Velocity (ft/s) vs. Residual Gas Holdup (%) – 12 ppm Frother

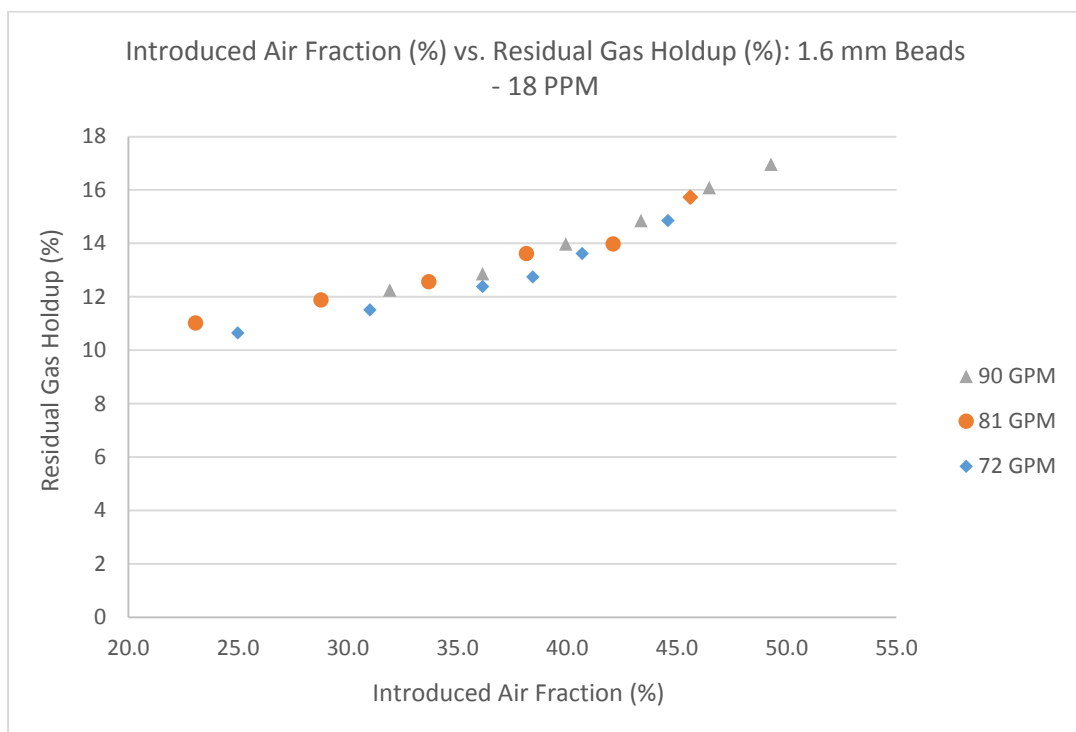


Figure 2-A. 1.6 mm Beads: Introduced Air Fraction (%) vs. Residual Gas Holdup (%) – 18 ppm Frother

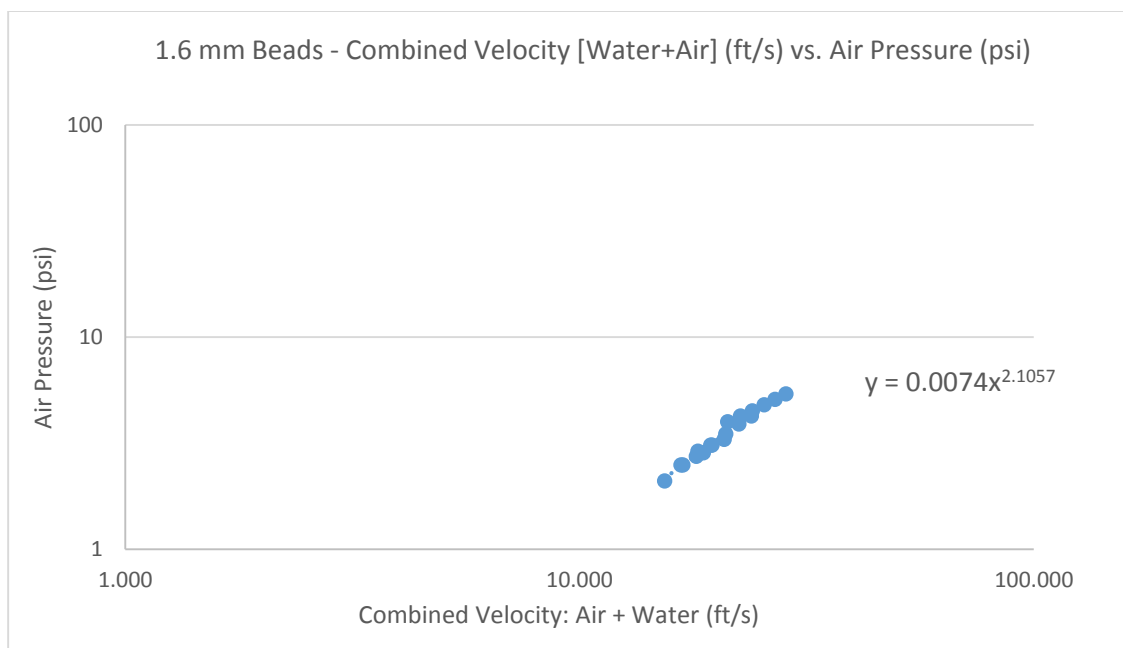


Figure 3-A. 1.6 mm Beads: Combined Velocity [Water + Air] (ft/s) vs. Air Pressure (psi)

APPENDIX B – 1.0 mm Bead Testing Program

Table I-B – Sparger Generated Gas Holdup Using 90 GPM Water and 1.0 mm Beads

2 in² - 90 Gal/Min (14.5 ft/s) Water - 1 mm Beads						
SCFM Air	Air Pressure (psi)	A + W Velocity (ft/s)	Air Fraction (%)	Gas Holdup - 12 PPM (%)	Gas Holdup - 18 PPM (%)	Bubble rise Velocity (ft/min)
10	5.7	28.57	49.47	16.46	18.19	11.11
9	5.4	27.07	46.66	14.85	16.46	11.23
8	5.15	25.59	43.58	13.62	14.35	11.79
7	4.9	24.14	40.18	12.25	13.49	10.81
6	4.6	22.69	36.36	11.38	12.25	10.10
5	4.4	21.28	32.14	10.51	11.38	8.77

Table II-B – Sparger Generated Gas Holdup Using 81 GPM Water and 1.0 mm Beads

2 in² - 81 Gal/Min (13 ft/s) Water - 1 mm Beads						
SCFM Air	Air Pressure (psi)	A + W Velocity (ft/s)	Air Fraction (%)	Gas Holdup - 12 PPM (%)	Gas Holdup - 18 PPM (%)	Bubble rise Velocity (ft/min)
9	4.6	25.369	48.8	15.72	16.09	11.66
8	4.2	23.879	45.6	14.85	14.85	11.17
7	4	22.468	42.2	13.12	13.99	10.24
6	3.75	21.060	38.3	12.25	13.12	9.14
5	3.5	19.670	33.9	11.01	11.88	8.26
4	3	18.261	28.8	9.78	11.01	6.68

Table III-B – Sparger Generated Gas Holdup Using 72 GPM Water and 1.0 mm Beads

2 in² - 72 Gal/Min (11.5 ft/s) Water - 1 mm Beads						
SCFM Air	Air Pressure (psi)	A + W Velocity (ft/s)	Air Fraction (%)	Gas Holdup - 12 PPM (%)	Gas Holdup - 18 PPM (%)	Bubble rise Velocity (ft/min)
8	3.6	22.261	48.1	13.62	15.22	10.88
7	3.25	20.832	44.6	12.75	14.35	9.91
6	3	19.451	40.6	11.88	13.12	9.22
5	2.75	18.087	36.1	11.01	11.88	8.35
4	2.5	16.742	31.0	9.78	11.01	6.87
3	2.5	15.444	25.2	8.41	10.15	5.18

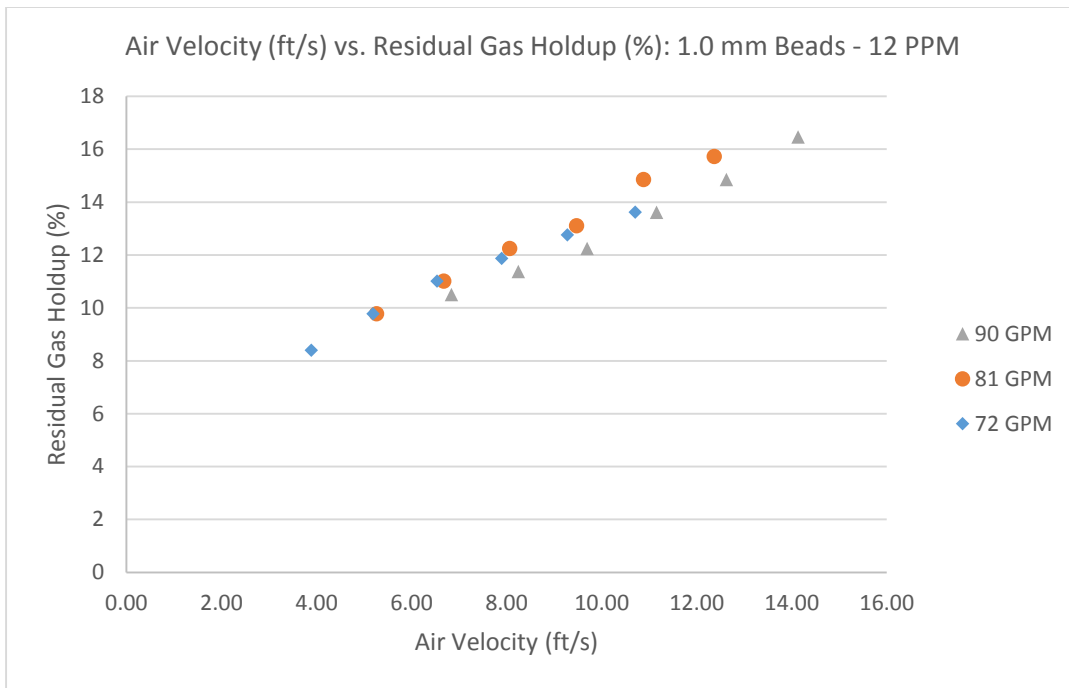


Figure 1-B. 1.0 mm Beads: Air Velocity (ft/s) vs. Residual Gas Holdup (%) – 12 ppm Frother

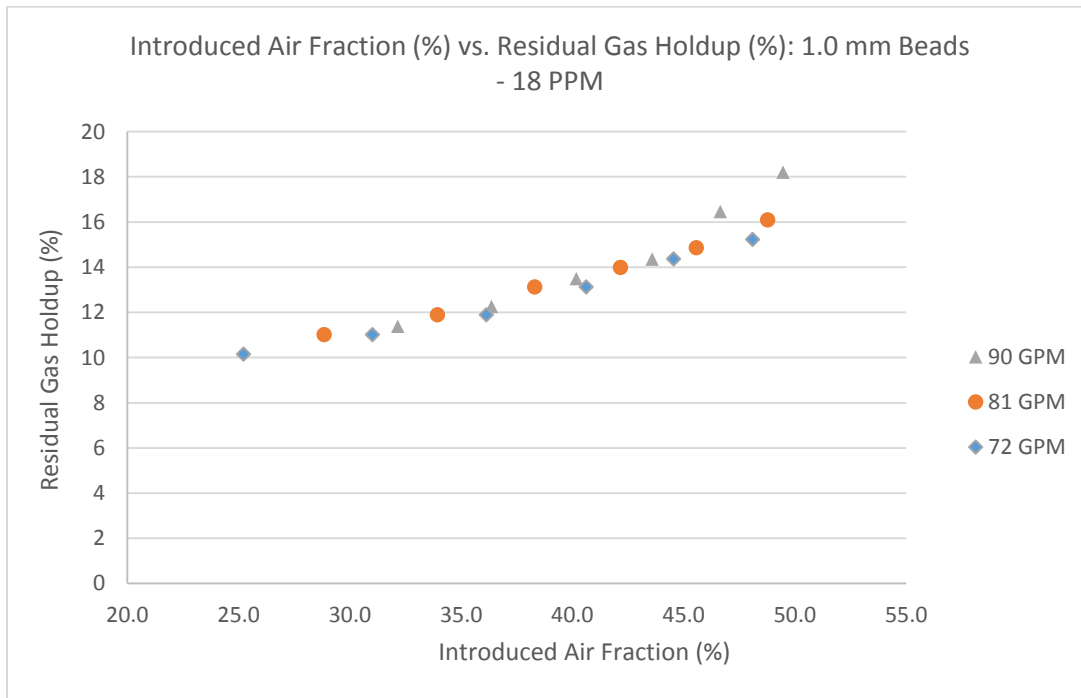


Figure 2-B. 1.0 mm Beads: Introduced Air Fraction (%) vs. Residual Gas Holdup (%) – 18 ppm Frother

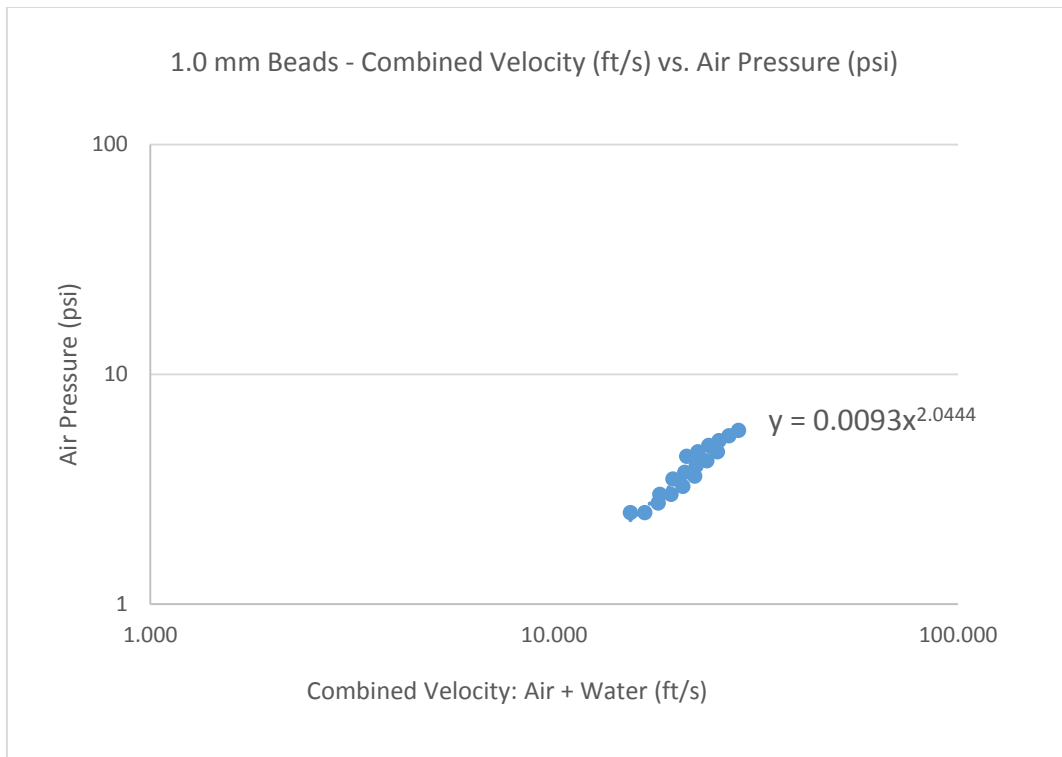


Figure 3-B. 1.0 mm Beads: Combined Velocity [Water + Air] (ft/s) vs. Air Pressure (psi)

APPENDIX C – No Magnetic Medium Testing Program

Table I-C – Sparger Generated Gas Holdup Using 90 GPM Water and No Beads

2 in² - 90 Gal/Min (14.5 ft/s) Water - No Beads					
SCFM Air	Air Pressure (psi)	A + W Velocity (ft/s)	Air Fraction (%)	Gas Holdup - 18 PPM (%)	Bubble rise Velocity (ft/min)
10	5.9	28.643	49.6	16.59	12.89
9	5.75	27.176	46.9	14.85	13.25
8	5.5	25.691	43.8	13.99	12.39
7	5.1	24.186	40.3	13.12	11.34
6	4.85	22.741	36.5	12.50	9.88
5	4.5	21.295	32.2	11.38	8.81

Table II-C – Sparger Generated Gas Holdup Using 81 GPM Water and No Beads

2 in² - 81 Gal/Min (13 ft/s) Water - No Beads					
SCFM Air	Air Pressure (psi)	A + W Velocity (ft/s)	Air Fraction (%)	Gas Holdup - 18 PPM (%)	Bubble rise Velocity (ft/min)
8	4.1	23.850	45.5	14.49	11.55
7	3.9	22.443	42.1	13.62	10.61
6	3.75	21.060	38.3	12.07	10.35
5	3.25	19.624	33.8	11.26	8.87
4	3	18.261	28.8	10.65	7.06
3	2.6	16.899	23.1	9.60	5.38

Table III-C – Sparger Generated Gas Holdup Using 72 GPM Water and No Beads

2 in² - 72 Gal/Min (11.5 ft/s) Water - No Beads					
SCFM Air	Air Pressure (psi)	A + W Velocity (ft/s)	Air Fraction (%)	Gas Holdup - 18 PPM (%)	Bubble rise Velocity (ft/min)
7	3.3	20.845	44.6	12.83	11.67
6	3.1	19.473	40.7	11.93	10.61
5.5	2.9	18.772	38.5	11.29	10.22
5	2.75	18.087	36.1	10.84	9.54
4	2.5	16.742	31.0	10.13	7.80
3	2.25	15.416	25.1	8.85	6.39

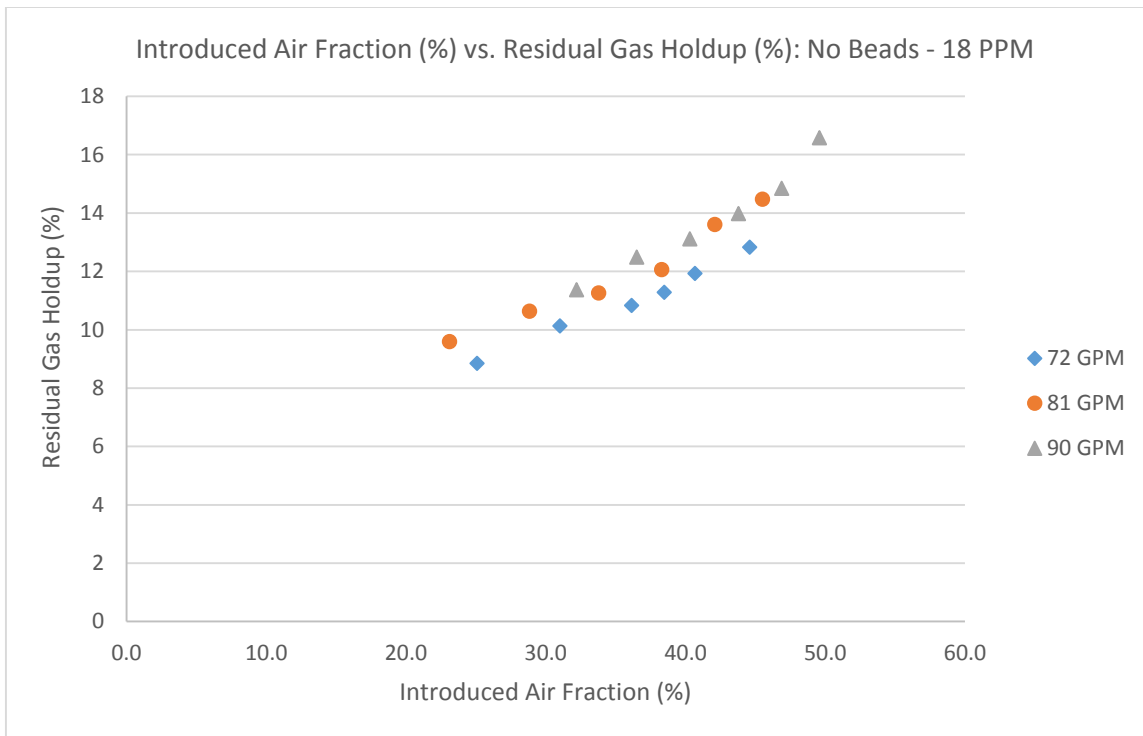


Figure 1-C. No Beads: Introduced Air Fraction (%) vs. Residual Gas Holdup (%) – 18 ppm Frother

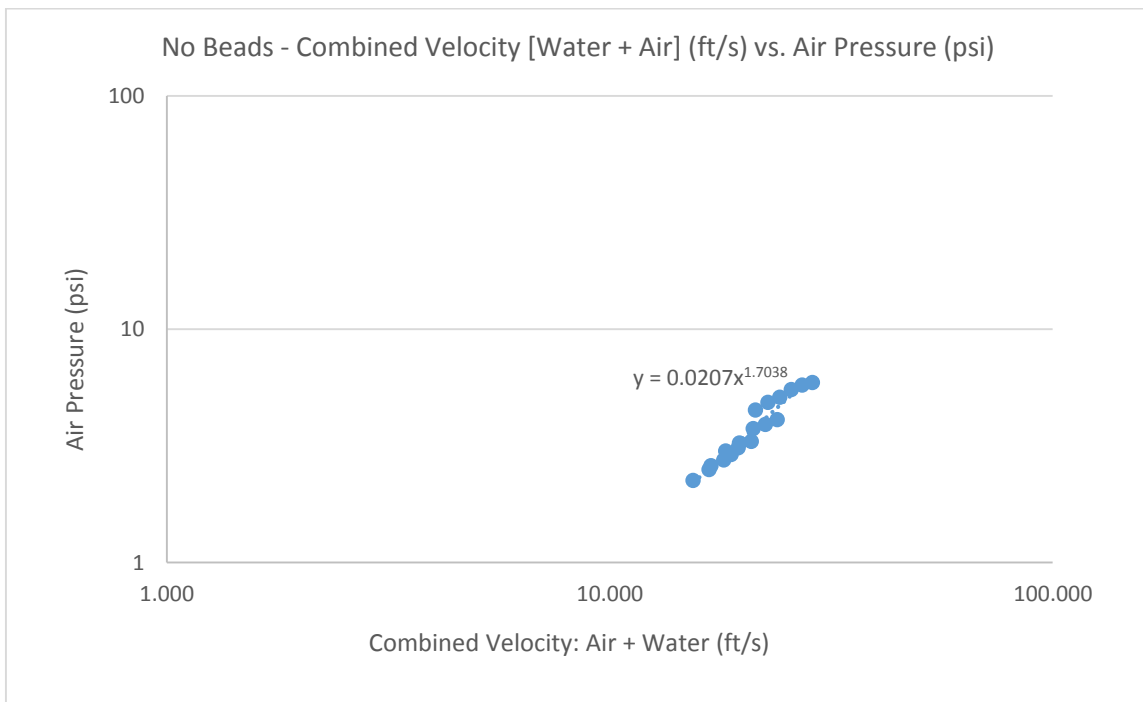


Figure 2-C. No Beads: Combined Velocity [Water + Air] (ft/s) vs. Air Pressure (psi)